Chemical Engineering Journal Advances 27 (2026) 101326

Contents lists available at ScienceDirect

Chemical Engineering Journal Advances

journal homepage: www.sciencedirect.com/journal/chemical-engineering-journal-advances

Recent progress in zeolite X synthesis from industrial waste

Božidar Ilić [a], Alenka Ristić [b,*], Saša Zeljković [a]

[a] Department of Chemistry, Faculty of Natural Sciences and Mathematics, University of Banja Luka, Mladena Stojanovića 2, 78 000 Banja Luka, Bosnia and Herzegovina
[b] Department of Inorganic Chemistry and Technology, National Institute of Chemistry, Hajdrihova 19, SI–1001 Ljubljana, Slovenia

ARTICLE INFO

Keywords:
Zeolite X synthesis
Industrial waste
Circular economy
Sustainability

ABSTRACT

Zeolite X, a low-silica aluminosilicate with notable adsorption and catalytic properties, can be synthesized from industrial waste materials in accordance with circular economy principles. This review examines recent studies on the production of zeolite X from coal fly ash (CFA), rice husk ash (RHA), granite stone sludge (GSS), ceramic waste, and other waste materials. We describe the relevant synthesis methods used in these studies, including pretreatment requirements to address compositional variability and impurity removal, as well as their influence on crystallinity and yield. This paper highlights successful applications in gas adsorption, toxic metal removal, and catalytic processes, among other uses, demonstrating performance comparable to conventional materials. The review also identifies promising but underexplored waste sources such as aluminum slag, silica fume, and biomass ash as potential alternative precursor and proposes future research directions to promote synthesis optimization, zeolite X modification techniques, industrial adoption, and targeted applications in environmental remediation and energy technologies.

1. Introduction

Zeolites are aluminosilicate materials characterized by a three-dimensional framework of aluminum and silicon tetrahedra interconnected by shared oxygen atoms. Their unique pore structures and precisely defined pore sizes enable a wide range of industrial and environmental applications [1]. The silicon (Si) and aluminum (Al) atoms in zeolites are centrally positioned, whereas the oxygen atoms are located at the corners and are shared between the tetrahedral units. This arrangement creates a system of pores and channels, which are essential for the adsorption and ion exchange capabilities of zeolites. The properties of zeolites depend on their composition and structural characteristics, particularly the Si/Al molar ratio. Based on this ratio, zeolite X is classified as a low-silica zeolite, with a molar ratio of <2 [2]. Zeolites are used in industrial applications because of their moderate pore size, high crystallinity, substantial surface area, and other favorable chemical properties. Zeolite X, in particular, is widely applied in gas purification systems, such as dehumidification during natural gas reforming, as well as in catalytic cracking processes [3].

Zeolite X, having a faujasite structure (Fig. 1). type, consists of sodalite cages that are associated with hexagonal prisms. The pores form of a 12-membered ring having a relatively large diameter of 0.74 nm. The inner cavity is 1.3 nm in diameter. The 14-hedron with 24 vertices, known as the sodalite cavity or β-cage, may be regarded as its principal building block. These β-cages are connected tetrahedrally at six-rings by bridging oxygen atoms to form double six-rings (D6Rs, hexagonal prisms), and, at the same time, an interconnected set of even larger cavities (supercages) accessible in three dimensions through 12-ring (24-membered) windows. The Si and Al atoms occupy the vertices of these polyhedra. The oxygen atoms lie approximately midway between each pair of Si and Al atoms but are displaced from these points to give near-tetrahedral angles about Si and Al. Single six-rings (S6Rs) are shared by sodalite and supercage and may be regarded as the entrances to the sodalite units. Each unit cell contains eight sodalite units, eight supercages, 16 D6Rs, 16 12-rings, and 32 S6Rs. Exchangeable cations that balance the negative charge of the aluminosilicate framework are found within the zeolite cavities. They are usually found at six different sites: site I at the centre of the D6R, I in the sodalite cavity on the opposite side of one of the D6Rs six-rings from site I, II inside the sodalite cavity near an S6R, II at the centre of the S6R or displaced from this point into a supercage, III in the supercage on a twofold axis opposite a four-ring between two 12-rings, and III somewhat or substantially off III (off the twofold axis) on the inner surface of the supercage [4,5].

The typical synthesis of zeolites and other mesoporous materials is not considered eco-friendly because of the use of organic templates as structure-directing agents [6]. To address these concerns and enhance

* Corresponding author.
E-mail address: alenka.ristic@ki.si (A. Ristić).

https://doi.org/10.1016/j.ceja.2026.101326

Available online 23 June 2026

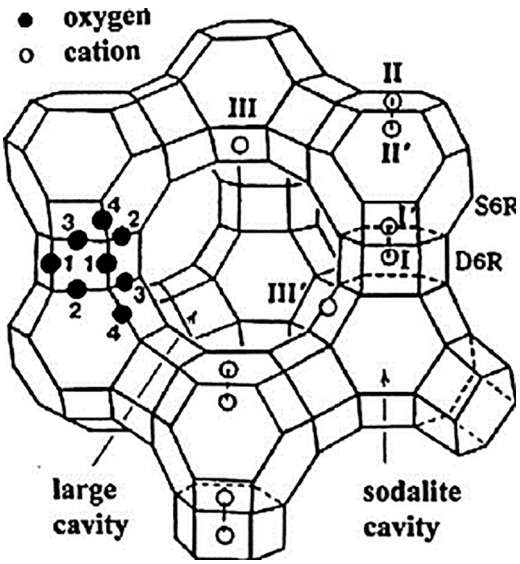

Fig. 1. The framework structure of zeolite X, near the centre of each line segment is an oxygen atom. The numbers 1–4 indicate different oxygen atoms. Si and Al atoms alternate at the tetrahedral intersections, except that Si substitutes for Al at about 4% of the Al positions. Extra-framework cation positions are labelled with Roman numbers. Reprinted from Journal of Catalysis, Vol. 244, Issue 2, Jince Sebastian, Krishna Mohan Jinka, Raksh Vir Jasra, "Effect of alkali and alkaline earth metal ions on the catalytic epoxidation of styrene with molecular oxygen using cobalt(II)-exchanged zeolite X", Pages 208–218, Copyright (2006), with permission from Elsevier.

the sustainability of zeolite X synthesis, recent efforts have focused on integrating the principles of green chemistry and green technology [7]. Green technology encompasses a broad array of innovative and sustainable strategies aimed at minimizing environmental harm by reducing waste, lowering energy demands, and avoiding toxic reagents. In the context of zeolite synthesis, this approach involves developing eco-friendly methods that eliminate or reduce the use of hazardous organic templates, favor water-based or solvent-free systems, and utilize renewable or waste-derived raw materials wherever possible. These advancements contribute to making the synthesis process more sustainable while maintaining or even improving material performance [7]. Moreover, traditional zeolite synthesis depends heavily on mineral resources and high-purity chemical reagents, which often results in significant economic and environmental costs [8]. Industrial waste is a growing environmental challenge, particularly because of the increasing global demand for materials and energy-intensive manufacturing processes [9]. Synthesis of zeolite X using various industrial and geological waste streams has emerged as a promising strategy within the framework of the circular economy. Instead of relying on virgin chemicals, waste materials rich in silicon and aluminum, such as fly ash, slags, and basalt powder, are being upcycled into high-value zeolites [10]. This not only reduces the environmental burden of waste disposal but also lowers the cost of zeolite production. For example, the reuse of post-reaction solutions from fly ash-based syntheses has been demonstrated to produce Na-X zeolites with high purity and surface area, closing the loop in the synthesis process [11]. Furthermore, zeolites derived from waste are being applied in catalytic processes to recycle plastics, contributing directly to sustainable material cycles and circular economy goals [12]. It has been demonstrated that zeolite X can be synthesized from industrial waste materials, enabling their recycling and repurposing [13]. A diverse range of industrial waste materials, including coal combustion waste [13–20], stone waste [21,22], agricultural waste [17,23], aluminum scraps, sand [3], waste porcelain [24], palm oil mill fly ash (POMFA), natural clay, and bentonite [2], has been successfully utilized for zeolite X synthesis. These waste materials are typically rich in silica (SiO_2) and alumina (Al_2O_3), the primary building blocks of zeolites, making them suitable precursors for hydrothermal or fusion-assisted synthesis methods [14].

The purpose of this review is to evaluate and promote the sustainable synthesis of Zeolite X from industrial waste materials as an environmentally and economically viable alternative to conventional raw materials, while identifying current challenges, research gaps, and future opportunities for industrial application. Recent studies on the synthesis of zeolite X from selected types of industrial waste are reviewed. Additionally, the potential applications of zeolite X derived from industrial waste are examined, with a focus on recent research related to applications of zeolite X.

2. Industrial waste used for zeolite X synthesis

Coal fly ash (CFA), a byproduct of coal combustion, is one of the most commonly used industrial wastes for the synthesis of zeolite X [18]. It is a complex industrial byproduct that contains various minerals, metal oxides, organic matter, and impurities, which poses significant challenges for its reuse. The combustion of pulverized coal in thermal power plants produces CFA as a fine and powdery byproduct. It is captured by electrostatic precipitators or bag filters before flue gases are released into the atmosphere. CFA primarily consists of SiO_2, Al_2O_3, iron oxide (Fe_2O_3), and calcium oxide (CaO), and its composition varies depending on the source of coal fly ash [25]. Despite its abundance, current utilization rates remain low. The main challenge in managing CFA is the lack of space for disposal, as a large area is needed, leading to increased financial costs for transportation and management [2]. Zeolite synthesis from CFA presents a promising solution, offering a pathway to high-value materials widely used in catalysis, adsorption, and separation processes. However, conventional synthesis methods often rely on pure chemical reagents, leading to high costs and inefficient resource use. Key challenges include enhancing the conversion efficiency of CFA to zeolites, improving the structural stability and regeneration of the resulting materials, and optimizing synthesis and modification protocols to increase adsorption performance and selectivity. The success of these efforts depends largely on the physicochemical properties of CFA, such as particle size, specific surface area, chemical composition and mineralogical structure [9,26,27]. The growing academic interest in the research of zeolite X is evident in the publication trends over the past 15 years. As illustrated in Fig. 2, the annual number of research articles dedicated to zeolite X has experienced a steady upward trajectory since 2010.

In addition to coal fly ash, another coal combustion waste used for zeolite X synthesis is coal-fired slag (CFS). Although it is visually different from CFA, it has also been successfully used for zeolite X synthesis [13]. Zeolite X synthesis using granite stone sludge (GSS), a type of stone waste, has also been reported [21]. The composition of GSS includes SiO_2, Al_2O_3, K_2O, CaO, Fe_2O_3, and other trace elements, indicating its suitability for zeolite X production [21]. Rice husk (RH) is one of the most abundant agricultural byproducts worldwide [23]. With an annual global rice production of approximately 571 million tons, approximately 140 million tons of RH waste are generated each year. While RH is primarily used as a fuel source or to provide nutrients in the soil, it is often discarded in the environment. As a renewable and sustainable carbon resource, RH has gained attention for its potential in synthesizing advanced materials for a variety of applications. It is a lignocellulosic biomass consisting of 28–30% inorganic matter and 70–72% organic matter. The inorganic fraction is mainly composed of SiO_2. In addition to its use as a fuel, RH and its ashes (RHA) have been extensively studied for their potential as adsorbents for removing heavy metals from wastewater. Research by Gargiulo et al. (2024) have also shown that, compared with untreated RH, materials derived from modified RH exhibit superior heavy metal adsorption properties [23]. Various methods, including combined pyrolysis/activation processes and surface modifications, have been explored to increase the

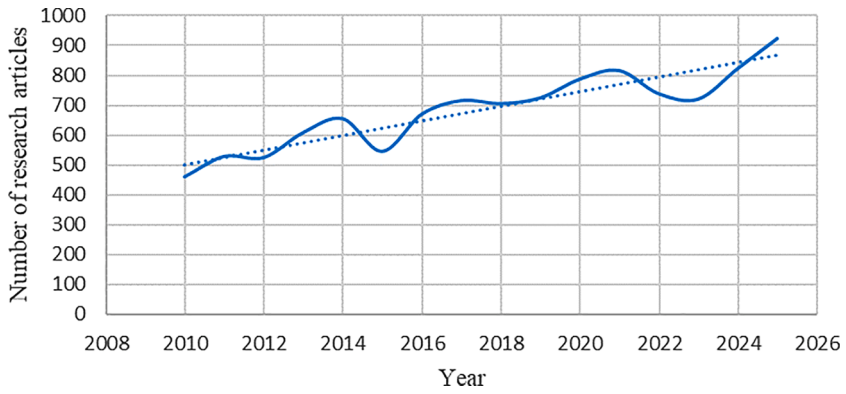

Fig. 2. Trend of zeolite X relevant research articles in the last 15 years (2010–2025). Data retrieved from OpenAlex on June 3, 2026. Figure created by the authors.

adsorption capacity of RH. A study by Jin et al. (2023) demonstrated that zeolite X can be synthesized from RHA and used in adsorption-related applications [17]. Another study by Chat et al. reported the synthesis of zeolite X from riceberry rice husk (RRH) for the purpose of propionic acid adsorption [28]. Unused fired products from the ceramic industry generate a significant amount of waste ceramics. While some of this waste is repurposed as artificial aggregates or raw materials for cement production or is used in other minor applications, a considerable portion is still disposed of at landfill sites. The limited capacity of these landfills poses notable social and environmental challenges. To address this issue, alternative methods for recycling ceramic waste have been explored. For example, an earlier study by Wajima and Ikegami (2009) reported the synthesis of zeolites from waste porcelain, demonstrating a promising approach for valorizing ceramic waste and reducing landfill dependence [24]. In addition to the above mentioned industrial waste, a wide variety of other wastes have been reported and considered for use in zeolite X synthesis, including POMFA [29], aluminum ash [30], crushed stone powder [30], begasse fly ash [2] and aluminum saline slag [2]. When narrowing the focus to the specific types of industrial waste utilized as silicon and aluminum sources, a clear preference emerges in the literature (Fig. 3). Ash (primarily coal fly ash) is by far the most heavily investigated industrial waste.

Silica fume and other compositionally similar waste materials are rarely used as a standalone precursor for Zeolite X because it consists of nearly pure, amorphous silicon dioxide with virtually no inherent aluminum content. Since Zeolite X is a faujasite-type (FAU) structure that strictly requires a low silicon-to-aluminum ratio between 1.0 and 1.5, utilizing silica fume forces researchers to add large amounts of external chemical aluminum sources, which reduces the economic viability of the waste-to-zeolite process. Furthermore, the extreme reactivity and ultra-fine particle size of silica fume cause it to dissolve rapidly in alkaline activators; this accelerated dissolution kinetics often bypasses the delicate nucleation window required for Zeolite X, thermodynamically driving the crystalline phase transformation toward denser, more stable impurities such as Hydroxysodalite, Zeolite P, or Analcime. Consequently, literature naturally favors pre-balanced aluminosilicate wastes like coal fly ash or kaolin clay over silica fume for target FAU-type zeolitization [31–33].

3. Synthesis methods using industrial waste

As shown in Table 1, various industrial wastes can serve as sources for the synthesis of zeolite X.

Methods for synthesizing zeolite X from industrial waste include hydrothermal synthesis, one-step and two-step hydrothermal synthesis,

Table 1
Industrial waste and methods of synthesis of zeolite X.

Industrial waste	Method of synthesis	Reference
Coal fly ash	Hydrothermal, microwave, ultrasound synthesis	[14–20]
Coal fired slag	Hydrothermal	[13]
Granite stone sludge	Alkali fusion hydrothermal	[21]
Rice husk ash	Hydrothermal	[17,23, 28]
Riceberry rice husk	Hydrothermal	[28]
Palm oil mill fly ash	Alkali fusion hydrothermal	[29]
Aluminum ash	Two-step hydrothermal	[30]
Crushed stone powder	Two-step hydrothermal	[30]
Begasse fly ash	Hydrothermal	[2]
Aluminum saline slag	Hydrothermal	[2,33]
Bituminous fly ash	Microwave	[34]

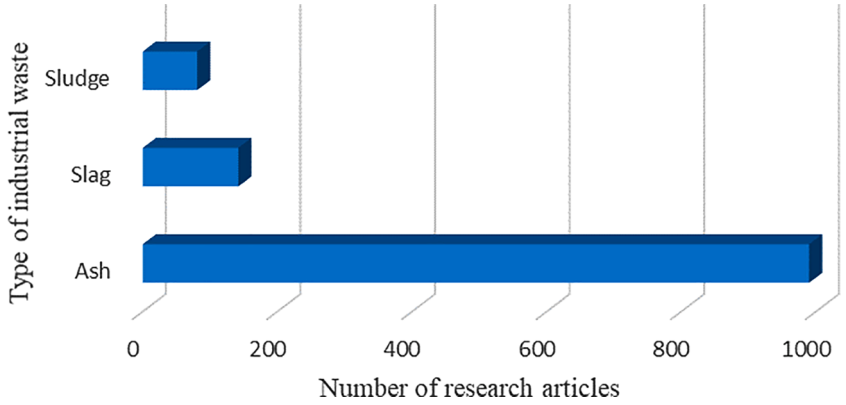

Fig. 3. Most researched industrial waste for zeolite x synthesis, based on OpenAlex data. Data retrieved from OpenAlex on June 3, 2026. Figure created by the authors.

alkali fusion-hydrothermal synthesis, microwave-assisted synthesis, ultrasound-assisted synthesis, ionothermal synthesis, mechanochemical synthesis, and sol-gel synthesis [8]. Hydrothermal synthesis enables the direct conversion of pretreated raw materials into zeolites. In this approach, pretreated materials are dissolved in an alkaline solution, typically sodium hydroxide (NaOH) or potassium hydroxide (KOH), facilitating the dissolution of silicates and aluminates. This is followed by an aging process under stirring, during which additional silica or alumina sources may be introduced to adjust the Si/Al ratio as needed. The resulting silica-aluminate gel is then subjected to hydrothermal crystallization in a sealed vessel. After crystallization, the zeolite product is recovered and typically undergoes drying or activation to remove water from the product [32].

Zeolite X has been successfully synthesized by hydrothermal method using various types of industrial waste materials (Table 1), including coal fly ash and slag [35]. Regarding the pretreatment of industrial waste for the hydrothermal synthesis of zeolite X, Bilgiç et al. (2023) reported that the raw materials, including fly ash and slag, possess high aluminum contents that are beneficial for zeolite formation, but they require appropriate treatment [35]. The materials were pretreated by grinding, sieving, calcination at 1073 K for 2 h, and acid leaching with 10% HCl to increase their reactivity and promote crystallization during synthesis. Marhoon et al. (2023) described the pretreatment of CFA to remove magnetic particles and acid washing of CFA using 20% HCl, with an acid-to-ash ratio of 20 $mL \cdot g^{-1}$. The mixture was subjected to continuous stirring at 300 rpm for 2 h at 363 K [36]. Following the treatment, the solid residue was filtered and thoroughly washed with deionized water until a neutral pH was achieved. The resulting sample was then dried overnight at 383 K. Magnetic separation was also performed in another study by Lee et al. (2024) to reduce the impurity content and increase the Si and Al contents in nonmagnetic fly ash (NMFA) [15].

Variations in hydrothermal synthesis include one-step hydrothermal synthesis, two-step hydrothermal synthesis, three-step activation and alkali fusion-hydrothermal synthesis. The one-step method is straightforward and low-cost, combining aging and crystallization in a single process, but may result in incomplete dissolution of waste material and lower product purity [8]. The two-step method improves the utilization of dissolved silicon and aluminum by separating initial hydrothermal treatment and crystallization, allowing adjustment of Si/Al ratios to enhance zeolite purity, although it requires additional reagents and precise reaction control. The three-step hydrothermal activation involves repeated cycles of aging, activation, and recycling of the product, improving conversion rates up to 80% and enabling reuse of materials, thus addressing some limitations of simpler methods. Moreover, the alkali fusion-hydrothermal method uses high-temperature fusion pretreatment to break down inert phases in waste material, significantly enhancing the reactivity and crystallinity of the zeolite; however, this method demands greater energy input and can generate byproducts. Each method balances the trade-offs between simplicity, efficiency, and scalability, with ongoing optimization aimed at sustainable industrial production [8]. In a recent study performed by de Aquino et al. (2020), zeolite X was synthesized using alkali fusion hydrothermal method. Two different CFA samples were used: one collected from electrostatic precipitators at a power plant and another obtained from silos exposed to flue-gas desulfurization. Before synthesis, the molar ratios in CFA were determined as follows: $SiO_2/Al_2O_3 = 3.5$, $Na_2O/SiO_2 = 2.05$, and $H_2O/Na_2O = 51.4$. CFA was fused with NaOH at 823 K for 1 h [18]. In another study by Tu et al. (2014), fusion was performed at a relatively high temperature and for a relatively long duration, i.e., 1120 K for 2 h [16]. Excessive alkali promotes the formation of hydroxysodalite, which is undesirable for the synthesis of zeolite X. The weight ratio of CFA to NaOH was 1:1. The goal of alkali activation is to dissolve the raw material, form reactive species, and direct the crystallization of zeolite X [19]. After sodium aluminate (Na_2AlO_3) was added, the homogenization process was performed under continuous agitation. Hydrothermal treatment was carried out at room temperature for 16 h [18]. Another study by Jin et al. (2023) demonstrated that zeolite X can be synthesized from RHA. A zeolite adsorbent was synthesized from coal ash and RHA using the alkali fusion-hydrothermal method. This study examined its optimal synthesis conditions, modifications, physical and chemical properties, and CO_2 adsorption capacity. The results revealed that the highest crystal purity and largest surface area were achieved when the $(SiO_2)_x \cdot (Al_2O_3)_y/NaOH$ weight ratio was 1:1.4 and the hydrothermal crystallization time was 12 h [17]. Additionally, zeolite X synthesis from waste porcelain using alkali fusion hydrothermal synthesis was reported earlier by Wajima and Ikegami (2009), where 10 g of ground waste porcelain with a particle size of 1 mm and SiO_2 and Al_2O_3 contents of 69.8 wt.% and 18.5 wt.%, respectively, was mixed with 12 g of NaOH powder, homogenized, and fused at a temperature of 873 K for 6 h. The material was then cooled to room temperature. The fused material was aged with vigorous agitation at room temperature for 24 h, followed by heating at 353 K for 12 h. Subsequent filtering, washing, and drying at 333 K produced zeolite X [24]. A different study from that of Kim et al. (2015) focused on the synthesis of zeolite A from ground windshield waste by acid treatment followed by hydrothermal processing. Although the primary objective was the formation of zeolite A, characterization of the product revealed the unexpected presence of the zeolite X phase in a sample that reacted for 48 h. These results open possibilities for further research into optimizing the use of glass waste specifically for zeolite X synthesis [37].

Zhao et al. (2025) described the synthesis and characterization of X-type zeolite from Fushun oil shale ash (OSA) and investigated its adsorption performance for Cd^{2+}. Unlike methods that utilize industrial waste pretreatments, this study directly used OSA without any pretreatment via the alkali fusion-hydrothermal method to simplify the process, lower costs, and prevent new pollution. Single-variable experiments were performed to optimize the preparation conditions. The resulting X-type zeolite (FSZ) exhibited high crystallinity at 89.98% with a specific surface area of 374.27 $m^2 \cdot g^{-1}$ [38].

Kongnoo et al. (2017), as previously stated, used palm oil mill fly ash (POMFA) as a waste material for zeolite X synthesis. Silica was extracted from POMFA, and the extraction process was described in the study. The samples were purified by washing, drying, sieving, and high-temperature calcination, followed by acid treatment with HCl to remove impurities and improve composition. The resulting material was further processed and used as a silica precursor for the synthesis of zeolite 13X. The selected method for zeolite X synthesis was alkali fusion hydrothermal synthesis. The molar ratio of SiO_2/Al_2O_3 was 3. The sample was fused with NaOH at different fusion temperatures (823 K, 873 K, 923 K, 973 K, and 1023 K) and held at these temperatures for 60–120 min. The fused material was then agitated at 135 rpm at room temperature for 24 h. Hydrothermal crystallization was carried out at 353 K for 12 h. The final product, with a pH near neutral, was acid-activated. Zeolite X and acid-treated zeolite X were compared. The results showed that acid activation, also known as dealumination of zeolites, had a significant positive effect on the mesopore and total pore volumes of zeolite X, and changes in surface morphology were observed. Analysis revealed that the acid-activated sample had a octahedral crystallites with a rough surface, whereas the nonacid-activated zeolite X exhibited octahedral crystallites with a smooth surface. Acid treatment also had a reducing effect on the yield of zeolite X, which was attributed to the removal of important inorganic materials [29]. Zeolite X was also successfully synthesized from stone waste and granite stone sludge, using alkali fusion hydrothermal method. A recent study by Mohammadi et al. (2025) described the synthesis and characterization of zeolite X from granite stone sludge. Sample from a stone-cutting factory was dried at 353–363 K for 72 h until its weight stabilized. NaOH was used as an activator for zeolite X synthesis. This synthesis involved acid modification with hydrochloric acid (HCl) and nitric acid (HNO_3). The initial experiment did not yield zeolite X from GSS, but after acid treatment to remove iron, zeolite X synthesis was successful. Following acid treatment, the sample was washed with distilled water

until the pH reached a neutral range. Twenty grams of acid-treated sample was mixed with 24 g of NaOH (at a ratio of 1:1.2) and calcined for 2 h in a furnace at different temperatures. The effect of calcination was observed at 673 K, 773 K, and 873 K. Zeolite X was detected at all temperatures, but analysis revealed the highest intensity at 673 K. This study emphasized that 673 K can be considered the optimal calcination temperature; however, lower temperatures were not investigated. The fused sample was mixed with deionized water and placed on a shaker for 24 h for homogenization. Crystallization was carried out at 363 K for 6 h. The prepared product was washed multiple times with deionized water to adjust the pH to 9–10. Characterization revealed that increasing the acid concentration during the acid treatment of granite stone sludge could lead to a decrease in sample crystallinity, which is a negative effect. Furthermore, the peak intensities increased with increasing aging time from 2 to 24 h, indicating that 24 h is the optimal aging time to obtain highly crystalline zeolite without impurity phases. Additionally, increasing the residence time in the furnace enhanced the degree of crystallization. Zeolite X with 100% purity was obtained under the following conditions: calcination at 673 K for 1 h, an aging time of 24 h, a residence time of 1 h, a GSS/NaOH ratio of 1:1.2, and crystallization at 363 K for 6 h. Further research is necessary to explore the potential of using different types of stone-cutting waste sludge for zeolite synthesis [21].

In addition to previous studies, zeolite synthesis from fly ash has been reported to use microwave (MW) [7,20,34] and ultrasonic (US) energies [7,39,40], resulting in improvements in the reaction time, crystal size, and product performance over those of conventional methods. Future studies are proposed to refine these techniques, including the combination of MW and US for CFA zeolitization, as well as scaling up to industrial levels for broader application [20].

Research by Truttim et al. (2023) described the MW synthesis of zeolite X from bituminous fly ash (BFA) and its characterization. BFA was collected from a power plant, mixed with a 3 M NaOH solution at a solid-liquid ratio of 1:25 and treated in a 1 L stainless steel reactor under continuous stirring at 500 rpm and a temperature of 343 K for 24 h. After the reaction, the solid residue was separated via filtration, and the clear filtrate was collected as the stock solution for subsequent zeolite synthesis. For the synthesis of zeolite X, the Si/Al ratio in the stock solution was adjusted to 3.0 by the addition of Na_2AlO_3. A 300 mL aliquot of the stock solution was combined with a Na_2AlO_3 solution prepared by dissolving 2.2 g of Na_2AlO_3 in 100 mL of NaOH solution, where the NaOH concentration ranged from 0 to 3.0 M. This mixture produced mixtures with final NaOH concentrations between 2.25 and 3.0 M. These mixtures underwent an aging process at ambient temperature for 24 h, followed by crystallization under microwave irradiation at temperatures between 338 K and 388 K, for durations ranging from 30 to 90 min. The resulting white precipitates were separated using vacuum filtration through GF/C filters (1.2 μm pore size) and subsequently washed with deionized water until the effluent pH stabilized near 10. Finally, the products were dried in an oven at 373 K for 12 h to yield zeolite X [34].

Experimental investigations conducted on three coal fly ash samples across a temperature range of 298–333 K demonstrated that the introduction of a one-hour ultrasonic pretreatment significantly lowered the temperature required for zeolite X crystallization. The ultrasonic treatment enhanced the dissolution of the aluminosilicate source material, rapidly inducing supersaturation with respect to the Al and Si species, which in turn promoted a high nucleation rate of the crystalline phases. This effect is attributed primarily to acoustic cavitation, which facilitates the formation of nucleation sites analogous to surface imperfections. Interestingly, while the Si/Al molar ratio of the fly ash strongly influenced the crystallization temperature during conventional synthesis, this dependency was considerably reduced when sonication was applied. The use of US pretreatment thus proved effective in enabling low-temperature synthesis of zeolite X regardless of the initial Si/Al ratio in the feedstock [40].

Alternative methods of synthesis include ionothermal synthesis, mechanochemical synthesis and sol-gel synthesis, among others. The ionothermal synthesis process involves selecting suitable precursors and dissolving them in an ionic liquid, followed by crystallization and recovery of the product. In contrast, sol-gel synthesis offers precise control over zeolite properties through the formation of a sol using metal alkoxides or salts, which undergo gelation via hydrolysis and condensation reactions. Thermal treatments such as drying and calcination promote crystallization and pore formation [8].

The mechanochemical method (MC) offers a rapid, energy-efficient route for synthesizing zeolite from industrial waste, enabling successful transformation within just 3 h under optimized conditions without the need for high-temperature treatment. Compared with conventional hydrothermal methods, the MC approach significantly reduces the synthesis time and particle size while improving the ion exchange capacity and Cd^{2+} adsorption performance of the resulting zeolite. Mechanochemical treatment through ball milling induces structural activation and enhances the reactivity of coal fly ash by breaking down stable phases such as quartz and mullite, thus facilitating the formation of P1 zeolite under milder conditions. Optimal synthesis was achieved at 403 K, 2 $mol \cdot L^{-1}$ NaOH, and a milling frequency of 30 Hz, yielding a zeolite product with a maximum Cd^{2+} adsorption capacity of 130.68 $mg \cdot g^{-1}$. By avoiding high-temperature fusion steps and reducing energy consumption, the MC method represents a scalable and sustainable alternative for valorizing coal fly ash into high-performance zeolitic adsorbents [41].

While alternative material synthesis strategies like ionothermal, mechanochemical, and sol-gel routes offer unique advantages, they are rarely used to synthesize Zeolite X from industrial waste. Ionothermal methods [8] rely on ionic liquids, while mechanochemical and sol-gel techniques struggle to yield the necessary crystalline uniformity and framework structure when faced with the complex chemical impurities and variable silicon-to-aluminum ratios inherent to raw waste materials. Consequently, scientific articles focus almost exclusively on hydrothermal synthesis. This method serves as the only practically relevant approach for waste utilization because its aqueous, highly alkaline environment efficiently dissolves the rigid aluminosilicate phases of the waste, enabling the reliable nucleation and growth of highly crystalline Zeolite X.

As shown in the Fig. 4, various industrial waste streams can be effectively upcycled into high-value Zeolite X (FAU framework), utilizing specific pretreatment and synthesis pathways tailored to the raw material's composition. Industrial waste including coal fly ash, rice husk ash, granite sludge, palm oil mill fly ash (POMFA), and porcelain/slag, undergo distinct pretreatment steps such as magnetic separation, acid leaching for iron removal, calcination, or alkali fusion to optimize the reactive silica and alumina phases. Following these adjustments, the conditioned precursors are subjected to hydrothermal crystallization techniques, ranging from classic hydrothermal aging to microwave- or ultrasound-assisted synthesis. Regardless of the disparate initial waste sources and processing routes, these pathways successfully yield Zeolite X characterized by a Si/Al molar ratio of 1.0 to 1.5, a specific surface area (BET) spanning 115 - 900 $m^2 \cdot g^{-1}$, and a distinct octahedral crystal morphology.

The development of crystalline zeolites from waste precursors relies heavily on the chosen synthesis vector, with each methodology presenting unique trade-offs between energetic inputs (Table 2), kinetic drivers, and product yields. While classic hydrothermal synthesis offers a low-cost, low-temperature framework (333–373 K), its reliance on slow surface attacks by aqueous alkali severely limits its efficiency, often yielding mixed phases with low BET surface areas over prolonged 24-hour periods. To overcome these kinetic barriers, advanced thermal and mechanical interventions are employed. Alkali fusion hydrothermal processing utilizes high-temperature roasting (823–1023 K) to convert inert quartz and mullite into highly soluble salts, ensuring complete matrix conversion and single-phase Zeolite X with exceptional crystallinity, though at the cost of high energy consumption. Alternatively,

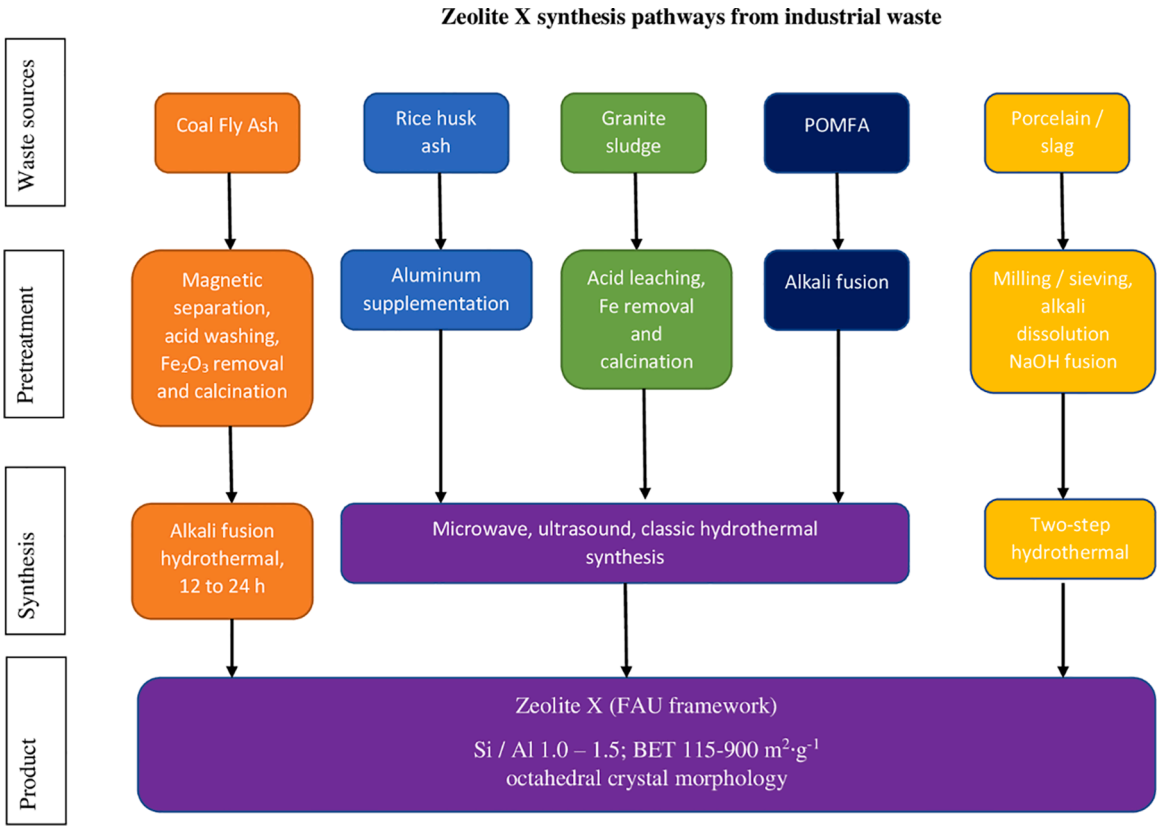

Fig. 4. A schematic diagram of selected synthesis pathways from different waste materials.

Table 2
Comparison of selected syntheses.

Method and waste source	Temp (K) and time	NaOH ratio	Pretreatment	Zeolite X purity and surface area ($m^2 \bullet g^{-1}$)	Ref
Alkali fusion hydrothermal using coal fly ash	333–363 (K); 12 – 24h	CFA:NaOH 1:1.2 (wt)	Magnetic separation of Fe impurities	Single phase; 425.9 $m^2 \bullet g^{-1}$	[15, 36]
Microwave assisted hydrothermal using bituminous fly ash	368 K 60 min	Extraction with 3 M NaOH	3 M NaOH leaching at 348 K for 24 h; Si/Al adjustment with $NaAlO_2$	91.8% purity; Surface area not specified.	[34]
Hydrothermal synthesis using fly ash	373 K 4h	3 M NaOH	Alkaline fusion at 1023 K for 1 h	Crystalline phase; 239.5 $m^2 \bullet g^{-1}$	[35]
Hydrothermal using coal fly ash	363 K 8 h	CFA:NaOH = 1:1.2 (wt)	Alkaline fusion at 1073 K for 2 h	High crystallinity; 487.6 $m^2 \bullet g^{-1}$	[42]
Ultrasound assisted hydrothermal using coal fly ash	333–368 K Fast, compared to conventional	Varies based on direct conversion vs. indirect fusion	Evaluated via direct conversion or indirect high-temperature fusion	Narrow crystal size distribution; high phase crystallinity; Enhanced microporous framework properties	[20]

decoupled hydrothermal loops isolate the extraction and crystallization stages to maximize surface areas and eliminate bulk impurities through precise stoichiometric adjustments, albeit using a more complex, multistage operational design. To mitigate the intensive thermal and structural demands of traditional frameworks, process intensification using wave and acoustic fields has emerged as a highly efficient alternative. Microwave-assisted synthesis leverages volumetric dielectric heating (2.45 GHz) and dipole-rotation-driven mass transport to drastically compress crystallization times to approximately 60 min, delivering high quantitative purity and narrow crystal size distributions. However, its industrial scale-up remains constrained by attenuation and penetration limits in dense slurries. Similarly, ultrasound and cavitation-assisted techniques utilize localized hotspots, mechanical shockwaves, and radical-induced polymerization to reduce gel aging times from hours to minutes, achieving exceptional spatial crystal dispersion and high relative crystallinity. While these dynamic synthesis pathways drastically accelerate dissolution and nucleation kinetics compared to classic hydrothermal aging, they require specialized reactor designs to mitigate severe equipment erosion, presenting an ongoing engineering challenge for industrial waste-to-zeolite conversion [20,34–37,42].

While traditional chemical syntheses often report product yields as a simple percentage, studies focusing on the synthesis of Zeolite X from complex industrial and consumer waste materials utilize multi-dimensional performance metrics instead. Because these waste precursors are highly heterogeneous and contain variable silicon and aluminum ratios alongside distinct impurities, a simple mass percentage fails to capture the true efficiency or success of the synthesis. Consequently, researchers quantify "yield" through specialized structural, qualitative, and functional indicators:

1. Phase Purity and Matrix Matching: Success is often defined by the ability to isolate pure crystalline phases (e.g., optimizing structural runs to separate Zeolite X from crystalline phases A and P) [13,16,30,34,36].

2. Functional Application Performance: Yield efficiency is frequently tied directly to the material's final application capacity. This includes measuring specific surface area paired with precise gas adsorption capacities [18,29,56,59].
3. Catalytic Activity Frameworks: In catalytic applications, the yield quality of the synthesized framework is evaluated by its operational output, such as providing optimal support for catalysts to achieve distinct hydrogen generation rates [35,36].
4. Thermal and Structural Stability: Yield optimization is also characterized by the stability of the pure crystal phase under specific thermal thresholds, where strict temperature controls are required during calcination to prevent adverse structural phase shifts [34,47,62].

Ultimately, studies demonstrate that the "yield" of Zeolite X synthesized from waste streams is comprehensively evaluated by crystal purity, structural integrity, and application-specific performance rather than standard gravimetric percentages [3,15,35,42,43].

To optimize the synthesis of Zeolite X from industrial waste, a careful trade-off between operational complexity, energy consumption, and reaction kinetics must be considered (Table 3). Classic hydrothermal synthesis remains highly favored for its simple operation and low instrumentation costs, yet it is severely bottlenecked by prolonged processing times and poor efficiency when breaking down inert waste minerals. To circumvent these mineralogical constraints, alkali fusion hydrothermal methods offer complete conversion of inert phases and exceptional product crystallinity, though this comes at the expense of high energy consumption during the high-temperature fusion stage. Alternatively, advanced kinetic enhancement techniques such as microwave- and ultrasound/cavitation-assisted synthesis have emerged to drastically accelerate the process, compressing crystallization and gel aging times down to approximately 60 min and mere minutes, respectively. However, these methods face practical engineering hurdles: microwave penetration attenuation limits scalability within dense industrial slurries, while ultrasound-assisted setups require specialized, costly reactors prone to equipment erosion.

4. Characterization and pretreatment of industrial waste and zeolite X

Characterization of industrial waste for zeolite X synthesis represents the first step in most of the examined studies. In a study by Boycheva et al. (2021), the chemical composition of coal fly ash was determined via atomic emission spectroscopy with an inductively coupled plasma excitation source and a spectrometer, whereas the phase composition and morphology of the ash particles were examined via X-ray diffraction (XRD) and scanning electron microscopy (SEM). Chemical analysis revealed that raw coal fly ash has high SiO_2 and Al_2O_3 contents, with notable variations in CaO, Fe_2O_3, and Na_2O contents, reflecting changes due to the synthesis process. The study also examined structural differences between coal fly ash from two different power plants. XRD and SEM revealed that one sample of coal fly ash contained predominantly cenospheres, whereas the other was composed mainly of agglomerates, highlighting significant structural differences [45]. These findings emphasize the importance of the detailed characterization of industrial waste materials, as their composition directly influences their morphology and suitability for zeolite synthesis. The study by Wajima and Ikegami (2009) described waste porcelain used for zeolite X synthesis as consisting of particles smaller than 1 mm, containing 69.8 wt% SiO_2 and 18.5 wt% Al_2O_3, with the remainder comprising Na_2O, K_2O, MgO, CaO, Fe_2O_3, and ZnO, as mentioned previously [24]. This highlights the relevance of detailed compositional analysis and particle size in evaluating waste materials for zeolite synthesis.

Hayfron et al. (2025) pretreated raw clay and prepared sodium silicate (SS) from rice husk. The raw clay was cleaned, suspended in distilled water, and subjected to sedimentation to isolate fine particles, followed by purification, drying at 378 K for 24 h, and calcination at 723 K for 4 h to remove organic and volatile impurities. SS was prepared from rice husk ash by washing, drying, and calcining the husks at 1073 K for 3 h, followed by acid activation with 0.1 M HCl, washing, drying, and alkaline treatment with 4 M NaOH; the mixture was then heated at 773 K for 1 h in a teflon-coated autoclave to yield the final SS precursor. These procedures ensure thorough preparation and characterization of the raw materials essential for synthesizing waste-derived Zeolite X [46].

Thorough characterization and pretreatment of diverse industrial waste materials, including coal fly ash, porcelain, and clay-based precursors, are critical steps that directly impact the quality and efficiency of Zeolite X synthesis. The desired properties of Zeolite X are largely determined by its intended applications. Its unique crystalline structure imparts important characteristics such as ion exchange capacity, adsorption ability, molecular sieving, and catalytic activity [47].

The chemical compositions of the waste precursors discussed in this review are summarized in tables 3 and 4. The data reveal significant variability in the SiO_2 and Al_2O_3 contents across waste types, which has direct implications for the synthesis strategy, pretreatment requirements, and achievable Zeolite X purity.

Coal fly ash (CFA) is the most widely studied precursor and has a relatively consistent Si/Al molar ratio in the range of 1.64–2.02 across samples from power plants in Bulgaria, Brazil, South Korea, and Thailand [15,18,34,45]. This range is close to the target Si/Al ratio of Zeolite X (< 2), making CFA inherently well suited for direct hydrothermal synthesis without major compositional adjustment. However, the absolute concentrations of SiO_2 and Al_2O_3 vary between sources (SiO_2: 49.96–60.76 wt%; Al_2O_3: 21.14–29.17 wt%), and the impurity profiles differ substantially. The iron oxide (Fe_2O_3) content ranges from 4.68 to 12.99 wt%, with the highest value recorded for CFA from TPP "AES Galabovo" [45]. Elevated Fe_2O_3 is particularly problematic, as iron species can substitute into the zeolite framework or precipitate as amorphous phases, reducing crystallinity and product purity; this effect was confirmed by FTIR analysis, which detected an additional absorption band at 660 cm^{-1} in zeolites synthesized from untreated CFA [36]. The CaO content also varies widely (1.54–9.63 wt%), and high CaO concentrations are associated with the formation of competing calcium silicate phases during hydrothermal synthesis. These findings collectively demonstrate that CFA cannot be treated as a compositionally uniform precursor: the synthesis protocol must be tailored to a specific ash source.

Granite stone sludge (GSS) presents a distinct compositional profile, with a pretreatment Si/Al ratio of 2.55 [21]. Notably, acid treatment with HCl and HNO_3, applied to remove iron impurities, results in a decrease in both SiO_2 (from 50.7 to 40.2 wt%) and the Si/Al ratio (from 2.55 to 2.15), accompanied by a marked increase in loss on ignition

Table 3
Main advantages and disadvantages of selected synthesis methods.

Synthesis method	Main advantage	Main Disadvantage	Ref
Classic hydrothermal	Simple operation; low instrumentation cost	Long processing hours; poor efficiency in breaking down inert waste minerals	[20, 37, 44]
Alkali fusion hydrothermal	Complete conversion of inert waste; excellent product crystallinity	Large energy consumption during the high-temperature fusion step	[35, 36]
Microwave Assisted	Drastic reduction in crystallization time (approx. 60 min)	Attenuation and penetration limit scale-up in dense industrial slurries	[20, 34]
Ultrasound/ Cavitation-Assisted	Compresses gel aging times from hours down to minutes via cavitation	Demands specialized reactors; potential issues with equipment erosion	[20, 44]

Table 4
Chemical composition of several waste precursors (Si/Al, impurities).

Waste type	SiO_2 wt%	Al_2O_3 wt%	Si/Al molar ratio	Key impurities (from highest to lowest wt%)	LOI wt%	Ref
CFA_{AES}	50.20	23.75	1.79	Fe_2O_3, CaO, MgO, SO_3, K2O, TiO_2, Na_2O, MnO, P_2O_5	2.16	[45]
CFA_{M3}	50.80	21.33	2.02	CaO, Fe_2O_3, K_2O, SO_3, MgO, TiO_2, P_2O_5, Na_2O, MnO	7.80	[45]
CFA_{JL}	60.76	25.48	2.02	Fe_2O_3, K_2O, CaO, TiO_2, MgO, Na_2O, SO_3, P_2O_5	1.33	[18]
CFA_{PE}	49.96	21.14	2.01	Fe_2O_3, CaO, MgO, Na_2O, K_2O, SO_3, TiO_2, P_2O_5	3.95	[18]
CFA_{SK}	56.20	29.17	1.64	Fe_2O_3, K_2O, others not specified	no data	[15]
Bituminous fly ash	53.60	25.40	1.79	CaO, Fe_2O_3, TiO_2, K_2O, MgO, P_2O_5, SO_3, Na_2O, SrO	no data	[34]
Rice husk ash	73.5	0.2	311.82	K_2O, P_2O_5, CaO, MgO, Fe_2O_3, Cl, Na_2O, CuO, ZnO	15.7	[48]
GSS_{BA}	50.7	16.9	2.55	Fe_2O_3, CaO, Na_2O, MgO, K_2O, TiO_2	1.8	[21]
GSS_{AT}	40.2	15.9	2.15	CaO, MgO, Na_2O, Fe_2O_3, TiO_2, K_2O	20.1	[21]
POMFA	50.57	1.03	41.66	CaO, K_2O, P_2O_5, MgO, Fe_2O_3, other	no data	[29]

CFA_{AES} - Coal Fly Ash (Boycheva et al. 2021) from TPP "AES Galabovo".
CFA_{M3} - Coal Fly Ash (Boycheva et al. 2021) from TPP "Maritza 3 Dimitrovgrad.
CFA_{JL} - Coal Fly Ash (de Aquino et al. 2020) from Jorge Lacerda power plant.
CFA_{PE} - Coal Fly Ash (de Aquino et al. 2020) from Pecém power plant.
CFA_{SK} - Coal Fly Ash (Lee et al. 2024) from power station in South Korea.
GSS_{BA} - Granite stone sludge before acid treatment (Mohammadi et al. 2025).
GSS_{AT} - Granite stone sludge after acid treatment (Mohammadi et al. 2025).
POMFA – POMFA (Palm oil mill fly ash), Kongnoo et al. 2017.

(LOI) from 1.8 to 20.1 wt%. The increase in LOI after acid treatment likely reflects the retention of surface hydroxyl groups and partially hydrated phases formed during leaching rather than residual organic matter. Importantly, acid treatment reduced the Fe_2O_3 content from 9.1 to 3.8 wt%, which Mohammadi et al. (2025) identified as the critical step enabling successful Zeolite X formation; synthesis without prior iron removal did not yield the target phase [21](Table 5).

The most compositionally extreme precursors are rice husk ash (RHA) and palm oil mill fly ash (POMFA), with Si/Al molar ratios of 311.82 and 41.66, respectively. Both materials consist predominantly of amorphous SiO_2 with negligible alumina content, which means that external aluminum sources must be introduced during synthesis to achieve the Si/Al ratio required for Zeolite X formation. While this adds a reagent cost and process step, the high silica purity of RHA - combined with low levels of iron and heavy metal impurities - may offer advantages in terms of final zeolite purity compared with that of CFA-derived materials, where contaminant management is more demanding. In contrast, POMFA contains 15.92 wt% CaO, the highest among all the precursors examined, which poses an additional challenge, as calcium phases may compete with Zeolite X crystallization during hydrothermal treatment.

Regarding the impurities` removal, acid leaching primarily functions to eliminate interfering mineral phases and reduce structural iron impurities. For example, washing coal fly ash or granite stone sludge with solutions of HCl or HNO_3 aggressively extracts iron oxides, which otherwise substitute deleteriously into the aluminosilicate framework or precipitate as amorphous clusters that stifle crystal nucleation [21,35,36]. Furthermore, targeted acid leaching reduces the concentration of calcium oxides, thereby suppressing the formation of competing calcium silicate hydrates that lower final zeolite yields [21,35]. Alkali fusion acts as a high-temperature thermal-chemical intervention (typically between 823 K and 1123 K) designed to dismantle inert crystalline phases like quartz and mullite inherent in waste residues [7,41]. By roasting the raw material with an activator like these, unreactive matrices are transformed into highly soluble, monomeric sodium silicate and sodium aluminate salts [18,41]. This rapid phase transformation bypasses the slow, surface-limited aqueous dissolution of traditional hydrothermal aging, generating a highly supersaturated gel that accelerates nucleation rates [7,40]. However, the alkali-to-waste ratio must be strictly controlled, as an excessive concentration of alkali shifts the framework thermodynamics, steering the phase selection away from the faujasite network of Zeolite X and toward denser, undesired hydroxysodalite phases [16]. Calcination provides a multi-fold advantage depending on the feedstock; when applied to biomass wastes like rice husk or raw clay, it efficiently vaporizes volatile organic impurities and removes bound structural water [46]. In stone-cutting sludges, calcination temperatures

Table 5
Impurities of several waste precursors in wt%.

Waste type	wt% of impurities									Other	Ref
	Fe_2O_3	CaO	MgO	SO_3	K_2O	TiO_2	Na_2O	MnO	P_2O_5		
CFA_{AES}	12.99	4.45	2.31	1.04	0.98	0.84	0.78	2.31	0.05	LOI 2.16	[45]
CFA_{M3}	4.68	9.63	0.82	0.86	2.17	0.78	0.37	0.09	0.49	LOI 7.80	[45]
CFA_{JL}	5.00	1.54	0.79	0.47	2.91	1.11	0.56	no data	0.07	LOI 1.33	[18]
CFA_{PE}	8.66	6.73	3.33	1.61	1.80	0.86	1.85	no data	0.14	LOI 3.95	[18]
CFA_{SK}	6.84	no data	no data	no data	0.83	no data	no data	no data	no data	no data	[15]
Bituminous fly ash	5.89	8.25	0.98	0.64	1.56	1.63	0.49	no data	0.97	SrO 0.19; etc. 0.38	[34]
Rice husk ash	0.8	1.3	1.1	no data	3.9	no data	0.4	no data	1.4	Cl 0.7; CuO and ZnO <0.1	[48]
GSS_{BA}	9.1	6.4	4.1	no data	3.9	0.7	6.3	no data	no data	LOI 1.8	[21]
GSS_{AT}	3.8	7.7	5.4	no data	0.7	0.7	5.4	no data	no data	LOI 20.1	[21]
POMFA	2.56	15.92	4.73	no data	8.45	no data	no data	no data	6.53	other 10.21	[29]

CFA_{AES} - Coal Fly Ash (Boycheva et al. 2021) from TPP "AES Galabovo".
CFA_{M3} - Coal Fly Ash (Boycheva et al. 2021) from TPP "Maritza 3 Dimitrovgrad.
CFA_{JL} - Coal Fly Ash (de Aquino et al. 2020) from Jorge Lacerda power plant.
CFA_{PE} - Coal Fly Ash (de Aquino et al. 2020) from Pecém power plant.
CFA_{SK} - Coal Fly Ash (Lee et al. 2024) from power station in South Korea.
GSS_{BA} - Granite stone sludge before acid treatment (Mohammadi et al. 2025).
GSS_{AT} - Granite stone sludge after acid treatment (Mohammadi et al. 2025).
POMFA – POMFA (Palm oil mill fly ash), Kongnoo et al. 2017.

directly influence the framework intensity. Observations show that while thermal activation at 673 K yields a highly reactive precursor optimal for high-intensity Zeolite X formation, elevating the calcination temperature beyond this threshold can lead to localized sintering and structural collapse, which reduces overall sample crystallinity [21]. Taken together, these data highlight that precursor composition is a primary determinant of synthesis complexity. Precursors with Si/Al ratios closest to the target value (CFA, GSS) require less compositional adjustment but demand more rigorous impurity removal, particularly for Fe and Ca species. Precursors with extreme Si/Al ratios (RHA, POMFA) require external component supplementation but may benefit from inherently lower contaminant loads. A systematic understanding of these compositional trade-offs is essential for selecting appropriate pretreatment and synthesis strategies for each waste source.

The characterization of Zeolite X synthesized from waste-derived precursors plays a crucial role in evaluating its structural integrity, physicochemical properties, and, importantly, its "sustainability-related" features. These features include defect density, thermal and hydrothermal stability, framework composition (particularly Si/Al ratio), and textural properties, all of which directly influence the material's performance in catalytic, adsorption, and ion-exchange applications [49].

Evaluating the structural evolution from heterogeneous waste matrices to highly crystalline Zeolite X requires an integrated multi-analytical approach to confirm framework integrity, morphology, and chemical states. XRD remains the primary technique for phase identification, phase purity validation, and relative crystallinity determination. Successful synthesis of Zeolite X is authenticated by the appearance of characteristic reflections corresponding to the cubic faujasite (FAU) topology, distinctly separating it from competing phases such as zeolite A, zeolite P, or hydroxysodalite. Peak intensities and full-width at half-maximum (FWHM) values are utilized to calculate crystalline size and track the complete consumption of amorphous quartz or mullite phases during hydrothermal conversion. FTIR is vital for functional group analysis and mapping the secondary building units of the aluminosilicate network. The characteristic infrared spectrum of Zeolite X features distinct absorption bands: asymmetric stretching of internal tetrahedra (typically around 1000–1050 cm^{-1}), symmetric stretching (660–750 cm^{-1}), and T–O bending vibrations (450–500 cm^{-1}). Crucially, the presence of a double-ring vibration band near 560 cm^{-1} serves as definitive evidence of the double six-ring (D6R) sub-structural units unique to the faujasite framework. FTIR is also highly sensitive to structural impurities; for instance, unremoved iron configurations introduce an anomalous absorption band at 660 cm^{-1}. XPS provides deep insight into the surface chemical states and coordination environments of elemental framework components. By mapping the binding energies of Si 2p, Al 2p, and O 1s orbitals, XPS tracks the successful incorporation of Al^{3+} ions into tetrahedral positions within the silica network, which generates the net negative framework charge balanced by exchangeable cations (e.g., Na^{+}). It further distinguishes framework elements from localized surface impurities or non-framework oxide residuals. Scanning Electron Microscopy (SEM) and Transmission Electron Microscopy (TEM) are essential for morphological and particle size evaluations. Well-crystallized Zeolite X typically manifests as distinct, well-defined octahedral crystals. Microscopic evaluations reveal that while non-acid-activated systems exhibit smooth crystal facets, post-synthesis acid modifications (dealumination) yield octahedral crystallites characterized by rougher, highly mesoporous surfaces. TEM further details the sub-micron pore alignment, verifying the presence of open micro/mesopore channel networks against structural blockages caused by unreacted waste aggregates.

A comprehensive characterization strategy integrates multiple complementary techniques to establish structure-property relationships. Powder XRD remains the primary method for confirming phase purity, crystallinity, and successful formation of the FAU-type framework characteristic of Zeolite X. It also enables semi-quantitative assessment of crystallization degree, which is closely linked to ion-exchange capacity and overall material performance [50]. Solid-state nuclear magnetic resonance (NMR), particularly ^{29}Si and ^{27}Al MAS NMR, provides detailed insight into the local framework environment. These techniques allow for the determination of Si/Al ratios, aluminium coordination states, and the presence of framework defects such as silanol nests or extra-framework aluminium species. Such defects are critical indicators of sustainability, as lower defect densities are typically associated with enhanced stability and longer operational lifetimes. Vibrational spectroscopic methods, including UV-Raman and FTIR spectroscopy, further complement structural analysis by probing framework vibrations, T-O-T (T = Si or Al) linkages, and the presence of hydroxyl groups or acid sites. Raman spectroscopy, in particular, is sensitive to short-range order and can detect subtle structural distortions or defect formation that may not be evident from XRD alone [51]. Textural properties are typically evaluated using nitrogen adsorption-desorption isotherms, enabling the determination of specific surface area by the Brunauer-Emmett-Teller (BET) method, as well as pore volume and pore size distribution. These parameters are essential for assessing the hierarchical porosity (micro- and mesoporosity) often targeted in waste-derived zeolites to enhance mass transport and adsorption efficiency [52]. Electron microscopy techniques, particularly high-resolution transmission electron microscopy (HRTEM) and SEM, provide direct visualization of crystal morphology, particle size, and the presence of structural defects or amorphous phases. HRTEM can additionally reveal lattice fringes and nanoscale disorder, offering valuable information on defect density and crystallographic coherence. Thermal and hydrothermal stability, key indicators of sustainable performance, are typically assessed using thermogravimetric analysis (TGA), differential thermal analysis (DTA), and in situ XRD under elevated temperatures or steam conditions. Waste-derived Zeolite X has been shown to exhibit high thermal stability and significant surface area, making it suitable for industrial applications such as adsorption and catalysis [53]. In recent years, advanced and operando characterization techniques have gained increasing importance. These approaches allow for real-time monitoring of structural and chemical changes under working conditions, providing deeper insight into degradation mechanisms, stability, and performance evolution [54].

Comprehensive characterization is vital to confirming the phase purity and morphological integrity of Zeolite X synthesized from various industrial wastes (Table 6). X-ray diffraction (XRD) and scanning electron microscopy (SEM) serve as the cornerstone diagnostic techniques across most synthesis pathways to verify crystallinity and the signature octahedral framework geometry. Advanced kinetic techniques, such as microwave and ultrasonic hydrothermal methods, yield high phase purity (e.g., 91.8% within 60 min) and highly uniform crystallite or spatial dispersions due to accelerated nucleation rates. Furthermore, chemical and thermal pretreatments strongly influence the final product structure; acid leaching of granite stone sludge to remove iron, combined with calcination at 673 K and a 24 h aging window, is required to eliminate amorphous impurity phases and maximize XRD peak intensity. Similarly, acid-dealuminated palm oil mill fly ash (POMFA) alters the final material's textural properties, resulting in octahedral crystallites with roughened surfaces and a substantial expansion in both mesopore and total pore volume.

Overall, the integration of these techniques enables a holistic evaluation of Zeolite X synthesized from waste materials, linking synthesis conditions to structural features and ultimately to performance. Such a multi-technique approach is essential for the rational design of sustainable zeolitic materials with optimized properties and reduced environmental impact.

5. Application of waste-derived zeolite

A wide range of environmental applications of Zeolite X derived from waste material has been reported (Fig. 5), including the removal of

Table 6
Correlation of synthesis vectors with characterization outcomes.

Waste Source and Synthesis type	Dominant Characterization Techniques	Key Structural Findings & Phase Outcomes	Ref
Coal Fly Ash (Alkali Fusion Hydrothermal)	XRD, SEM, FTIR	Single-phase FAU network; prominent 560 cm^{-1} double-ring FTIR bands; defined octahedral morphology. Fe impurities yield a 660 cm^{-1} band if unseparated.	[15, 36]
Bituminous Fly Ash (Microwave Hydrothermal)	XRD, Particle Size Analysis	91.8% phase purity achieved rapidly within 60 min; highly uniform crystallite size distribution.	[34]
Coal Fly Ash (Ultrasonic Hydrothermal)	XRD, SEM	Accelerated nucleation rates via acoustic cavitation; uniform spatial crystal dispersion under low-temperature conditions.	[20, 40]
Granite Stone Sludge (Acid-Leached Fusion)	XRD, SEM, Compositional Profiling	100% pure Zeolite X obtained only after iron removal; calcination at 673 K yields optimal peak intensity; longer aging (24 h) eliminates amorphous impurity phases.	[21]
Palm Oil Mill Fly Ash (Alkali Fusion Hydrothermal)	SEM, Porosimetry, Morphological Profiling	Acid-dealuminated samples show octahedral crystallites with rough surfaces alongside a dramatic expansion in mesopore and total pore volume.	[29]

contaminants, specifically heavy metals, cations, anions, and organic contaminants, including radioactive substances. Additionally, the catalysis and adsorption potential are examined [55]. Research by Wang et al. (2025) emphasized the use of spent fluid catalytic cracking catalysts for Zeolite X synthesis. This study presents a novel low-temperature activation method for spent fluid catalytic cracking (SFCC) catalysts, enabling their conversion into high-quality Zeolite X (SFCC-X-200) under mild hydrothermal conditions. The synthesized zeolite exhibited excellent crystallinity, high CO_2 adsorption capacity, and superior selectivity for CO_2/CH_4 and CO_2/N_2 separation, outperforming conventional materials. These results highlight SFCC-X-200 as a cost-effective, sustainable solution for industrial CO_2 capture and separation [56].

A study by He et al. (2024) highlighted the potential of Zeolite X in advanced composite materials, demonstrating its effectiveness when used as a core in a shell-core structured adsorbent for adsorption heat pump (AdHP) systems. Although Zeolite X in this case was not derived from waste, the demonstrated thermal stability, water regulation, and energy-saving performance suggest that similarly structured materials synthesized from industrial waste could offer comparable benefits in sustainable energy and gas separation applications [57]. A recent study by Lee et al. (2024) demonstrated the successful upcycling of coal fly ash into high-performance zeolitic adsorbents for ammonia gas removal. Among the synthesized materials, Zeolite X, derived from coal fly ash using NaOH, exhibited outstanding adsorption capacity (64.91 $mg \cdot g^{-1}$) and excellent recyclability (92% efficiency after five cycles), outperforming even commercial zeolite 13X. These results highlight the potential of coal fly ash-derived Zeolite X as a cost-effective and energy-efficient alternative for gas purification applications [15].

Another recent study by Feudjio et al. (2025) involving Na-X zeolite synthesized from clay demonstrated that ion exchange with K^+, Mg^{2+}, and Ca^{2+} ions can significantly alter the water adsorption properties of the material. Despite minimal structural changes post-exchange, notable modifications in surface area and pore volume were observed, which were attributed to cation-induced pore blockage. In particular, Zeo-Mg-

Fig. 5. Reported applications of waste-derived zeolites. The figure was improved with the help of OpenAI.

X and Zeo-Ca-X exhibited enhanced water adsorption performance and good hydrothermal stability, highlighting the potential of modified waste-derived zeolites in humidity control and adsorption-based applications [58].

Zeolite X synthesized from industrial waste sources such as fly ash and slag has been investigated as a low-cost catalyst support for Co–B catalysts in $NaBH_4$ hydrolysis for hydrogen generation (Bilgiç et al., 2025). The catalysts, prepared via impregnation and chemical reduction, exhibited promising hydrogen production rates and good reusability. The performance of these systems was influenced by the physicochemical properties of the zeolite supports, particularly the Si/Al ratio and surface characteristics. These findings highlight the potential of waste-derived Zeolite X as an efficient and economically viable material for on-demand hydrogen production, with applications in portable proton exchange membrane fuel cells [35].

The adsorption behaviors of NO, NH_3, SO_2, CO_2, and C_7H_8 from flue gases on waste-derived Zeolite X were explored by Dai et al. (2025), and successful conversion of coal fly ash into high-performance Zeolite X adsorbents via optimized calcination and hydrothermal treatment was demonstrated, resulting in an elevenfold increase in the specific surface area. The synthesized zeolite exhibits selective adsorption of various flue gas components, with maximum adsorption capacities at 293 K reaching 1.58 $mmol \cdot g^{-1}$ for NH_3 and 1.16 $mmol \cdot g^{-1}$ for SO_2, significantly exceeding those for other gases such as CO_2, C_7H_8, and NO In situ diffuse reflectance infrared Fourier transform spectroscopy (DRIFTS) analysis, combined with density functional theory (DFT) calculations, revealed that bridged oxygen bonds (T-O-T) within the zeolite framework act as primary adsorption sites. These sites facilitate electron transfer through exothermic interactions with gas molecules, increasing the adsorption efficiency. These findings establish a sustainable approach for the simultaneous treatment of solid waste and flue gas pollutants from coal-fired power plants while providing molecular-level insights to guide the rational design of waste-derived zeolite adsorbents for multipollutant control applications. Future research should focus on optimizing the selective adsorption properties and evaluating the long-term stability of these materials under industrial operating conditions [42].

The comparative data in the Table 7 highlights a profound operational distinction between the synthetic benchmark and the waste-derived alternative when subjected to consecutive thermal regeneration cycles. Although the commercial 13X zeolite initially exhibits a superior baseline adsorption capacity due to its optimized structural purity and high concentration of accessible microporous acid sites, it suffers from severe, irreversible thermal degradation under repeated handling, retaining a mere 31.5% of its functionality by the fifth cycle. In stark contrast, the fly ash-derived zeolite framework demonstrates exceptional structural robustness and thermal resilience, maintaining an impressive 92.0% recycling efficiency across the same evaluation span. This stark divergence in longevity underscores a critical trade-off where the waste-derived zeolite compensates for its marginally lower initial capture performance by dramatically outperforming the commercial baseline in cyclic stability, establishing itself as a far more viable and sustainable candidate for long-term industrial gas purification and circular-economy engineering.

The study by Marhoon et al. (2023) aimed to evaluate the effects of coal fly ash (CFA) pretreatment, optimize synthesis parameters, characterize the resulting Zeolite X properties, and assess its efficiency in removing the heavy metal ions Ni^{2+} and V^{5+} under various conditions. Magnetic separation was applied to remove magnetic impurities from raw coal fly ash. Acid washing of raw CFA effectively reduced undesirable metal oxides, with XRF analysis revealing a pollutant oxide content $<12\%$ in treated CFA. XRD confirmed that under optimal synthesis conditions (12 h, 363 K), TCFA yielded high-purity, single-phase Zeolite X, unlike the less pure zeolite derived from RCFA. BET surface area analysis revealed a significantly greater specific surface area for TCFA-derived Zeolite X (452 $m^2 \cdot g^{-1}$) than for RCFA-derived Zeolite X (115 $m^2 \cdot g^{-1}$). SEM images revealed that Zeolite X-TCFA possessed enhanced crystallinity and purity with well-defined crystals, whereas Zeolite X-RCFA displayed signs of impurity intergrowth. FTIR further confirmed these observations, with an additional peak at 660 cm^{-1} in Zeolite X-RCFA, indicating that contaminant phases were absent in the TCFA sample. Adsorption experiments for Ni^{2+} and V^{5+} ions demonstrated the influence of initial concentration, contact time, zeolite dosage, and pH on removal efficiency. Kinetic analysis favored the pseudo-second-order model, suggesting that chemisorption was the dominant adsorption mechanism. Isotherm studies revealed that the Langmuir model better described the adsorption process than the Freundlich model did, indicating monolayer adsorption on a homogeneous surface. Overall, this research highlights the difference between raw and treated CFA for Zeolite X synthesis and emphasizes the production of environmentally friendly and cost-efficient adsorbents for heavy metal remediation [36].

Zeolite X synthesized from riceberry rice husk (RRH) was effectively utilized for propionic acid adsorption in a study by Na Chat et al. (2022). Among the synthesized samples, the zeolite treated with 0.5 M HCl (0.5HCl-X) presented the highest adsorption capacity, reaching 516 $mg \cdot g^{-1}$ after 30 min of equilibration. Kinetic analysis indicated that the adsorption followed a pseudo-second-order model, suggesting that chemical adsorption governed the rate-controlling step. This work further demonstrates the versatility of waste-derived Zeolite X materials as efficient adsorbents, complementing other studies where Zeolite X from CFA, slag, and rice husk precursors has been successfully applied for removing diverse pollutants, such as heavy metals, gases, and organic acids. Collectively, these findings highlight the potential of converting agricultural and industrial wastes into valuable zeolite adsorbents for environmental remediation and catalytic applications [28].

Waste-derived Zeolite X has exceptional versatility and efficiency across a broad spectrum of environmental applications, including heavy metal and organic contaminant removal, gas adsorption, catalysis, and energy-related processes. Studies consistently show that converting industrial and agricultural wastes into Zeolite X not only provides cost-effective and sustainable materials but also often enhances the adsorption capacity, selectivity, and catalytic performance compared with those of their conventional counterparts. These advances underscore the significant potential of waste-derived Zeolite X as a green solution for pollution control, resource recovery, and clean energy technologies.

Table 7
Adsorption related data of selected studies.

Zeolite X variant	Adsorption conditions	Gas Species	Adsorption capacity	Reference
Commercial Li-H-X Zeolite	Static: 298 K, 20 bar	CO_2	9.6 $mmol \cdot g^{-1}$	[59]
		H_2	0.78 $mmol \cdot g^{-1}$	
Zeolite X from Bottom Ash modified with polyethyleneimine	Thermogravimetric: 348 K, 1 bar	CO_2	0.97 $mmol \cdot g^{-1}$	[60]
Zeolite X from Fly Ash	Dynamic Flue Gas Simulation: 293.15 K, 1000 ppm feed for NH_3, 1500 ppm feed for SO_2, 400 pm feed for NO	NH_3	1.58 $mmol \cdot g^{-1}$	[42]
		SO_2	1.16 $mmol \cdot g^{-1}$	
		NO	0.38 $mmol \cdot g^{-1}$	
Zeolite X from non magnetic fly ash	Dynamic streams: 303.15 K, 1 bar total pressure	NH_3	3.81 $mmol \cdot g^{-1}$	[15]

6. Future challenges and perspectives

Currently, several waste materials are actively being considered for the synthesis of Zeolite X [61]. Waste materials such as fly ash [17,28, 35,45], slag [13,35], or agricultural residues [17,23,28] vary widely in composition and impurities, which can affect reproducibility and zeolite quality. The development of robust pretreatment and standardization protocols is essential to ensure consistent synthesis outcomes. Translating laboratory-scale synthesis methods to large-scale, cost-effective, and energy-efficient industrial processes remains challenging. Optimizing synthesis parameters to reduce energy consumption, synthesis time, and waste generation is critical [7,62].

Coal fly ash and other waste materials may contain hazardous elements (e.g., toxic metals) [63], raising concerns about the final zeolite product's safety and environmental impact. The effective removal or immobilization of such contaminants is needed for safe applications. Achieving precise control over Zeolite X's physicochemical properties (e.g., pore size, ion-exchange capacity, crystallinity) through waste-derived synthesis routes can be difficult but is necessary to optimize performance for specific applications. Ensuring that waste-derived Zeolite X maintains structural integrity, adsorption capacity, and catalytic activity under real industrial conditions over extended use is a key challenge that requires further study.

The use of waste materials to produce high-value Zeolite X supports resource recovery and waste minimization, advancing sustainable material cycles and reducing the environmental footprint [8]. Combining waste-derived Zeolite X with modification techniques such as ion exchange can tailor properties to emerging applications in gas separation, catalysis, and energy storage [40,58]. Waste-derived zeolites may be integrated into innovative systems such as adsorption heat pumps [57], membrane reactors for thermocatalytic conversion of CO_2 [64] or fuel cells [43,65], broadening their practical utility. Employing data-driven approaches [66] to predict optimal synthesis conditions and performance on the basis of variable waste feedstock composition could accelerate development and industrial adoption. The development of standards and certifications for waste-derived zeolite materials could increase market acceptance, safety, and reliability, while promoting commercial use. Waste-derived Zeolite X has attracted significant attention due to its wide range of current and potential applications in environmental remediation, gas separation, catalysis, ion exchange, and energy-related technologies. One of its most extensively investigated applications is wastewater and water treatment, where its high adsorption capacity enables the efficient removal of heavy metals such as Pb^{2+}, Cd^{2+}, and Cu^{2+}, as well as ammonium ions, organic dyes, and radioactive contaminants [15,36,38,67]. Owing to its low production cost and the abundance of waste-derived precursors, Zeolite X is particularly promising for the development of affordable adsorbents in developing countries, decentralized water purification systems, and advanced hybrid membrane–zeolite treatment technologies [9,55]. Another rapidly growing field is gas separation and carbon capture. The unique pore structure and high surface area of Zeolite X enable the selective adsorption of gases including CO_2, H_2S, SO_2, and CH_4, making it suitable for flue gas treatment, biogas purification, natural gas upgrading, and hydrogen purification processes [18,42,45,56,60]. With increasing global efforts to reduce greenhouse gas emissions, waste-derived Zeolite X is emerging as a cost-effective alternative to conventional adsorbents for industrial-scale carbon capture and storage applications [17,62]. In the field of catalysis, Zeolite X has demonstrated considerable potential in petroleum refining, catalytic cracking, biomass conversion, and biodiesel production [6,10,12]. Furthermore, modification of Zeolite X with transition metal ions can enhance its catalytic activity, thermal stability, and reaction selectivity, expanding its applicability in green fuel synthesis, plastic waste valorization, and renewable energy technologies. These developments highlight the versatility of Zeolite X as a catalyst for sustainable chemical processes [4,12,35]. The ion-exchange properties of Zeolite X also contribute to its technological importance. Its ability to exchange cations such as Na^+, Ca^{2+}, Mg^{2+}, and NH_4^+ makes it valuable for water softening, nutrient recovery, soil amendment, and nuclear waste remediation. Such applications further support the role of waste-derived Zeolite X in promoting circular economy principles and sustainable resource management [9, 55,71,72]. More recently, research has explored the incorporation of Zeolite X into energy storage systems, including supercapacitors, battery separators, and thermal energy storage materials [1,57]. Although these applications remain at an early stage of development, they indicate promising future opportunities for waste-derived Zeolite X in sustainable energy technologies, smart environmental materials, and advanced sensor systems. Collectively, these diverse applications demonstrate that waste-derived Zeolite X is evolving from a low-cost adsorbent into a multifunctional material with significant potential to address environmental, energy, and industrial challenges.

Further, it is necessary to explore underutilized wastes such as aluminum saline slag [2,67], silica fume [31,68] and ceramic waste [24]. These waste materials show promise but need further investigation. Biomass ash [69] could be investigated for high-purity Zeolite X. The optimization of synthesis for industrial adoption and the development of AI-driven models [70] to predict optimal synthesis conditions constitute the next step in applying the current knowledge for the benefit of the environment. Expanding the potential applications of waste-derived Zeolite X in membrane reactors (e.g., for CO_2 conversion), adsorption heat pumps, and fuel cells, alongside investigating surface modifications such as metal doping and acid activation to increase selectivity, represents a key priority for future research.

Waste-derived Zeolite X has strong opportunity in water treatment, gas separation, catalyst support, and circular-economy applications because it combines low-cost feedstocks with high cation-exchange capacity and useful pore structure. Its main industrial appeal is that waste streams such as fly ash, biomass ash, and other industrial residues can be turned into higher-value materials instead of being landfilled [71,72].

The biggest challenge is feedstock variability: waste composition changes by source, season, and preprocessing route, which makes product quality harder to standardize. Impurities and unstable chemistry can reduce crystallinity, phase purity, and performance, especially when compared with conventionally synthesized zeolites.

There is a clear market opportunity in wastewater treatment for metals, ammonia, phosphates, and dyes, where Zeolite X can be cost-effective and regenerable. Beyond water treatment, waste-derived Zeolite X can be adapted for gas separation, volatile organic compound adsorption, agriculture, and industrial catalysis, which broadens its commercial relevance. A further opportunity is coupling zeolite production with carbon and waste-reduction goals, since it supports resource recovery and circular economy strategies.

Industrial scalability will depend on three things: reliable waste preprocessing, simpler synthesis routes, and proof that the full process is economically and environmentally favorable. The most scalable pathways are likely to use abundant, homogeneous wastes, low-temperature or low-chemical synthesis, and closed-loop recovery of reagents and water. Successful commercialization will also require quality control standards so that waste-derived Zeolite X can compete with conventional materials in adsorption capacity, durability, and regeneration.

In practice, waste-derived Zeolite X is most likely to scale initially in niche industrial applications where the feedstock is local, performance requirements are well defined, and the cost advantage is clear. Broader adoption will follow only if manufacturers reduce variability and demonstrate stable product specifications at pilot and full scale.

Regarding future directions, the following can be concluded:

- Greener synthesis methods: research is moving towards lower-energy, lower-waste routes such as solvent-free, microwave-assisted, and fusion-based methods.

- Better feedstock control: future work will likely focus on achieving more consistent product quality despite variability in waste composition.
- Higher-value applications: beyond basic adsorption, waste-derived Zeolite X is expected to expand into gas separation, CO_2 capture, ion exchange, and composite materials.
- Scale-up and economics: the key challenge is progressing from laboratory synthesis to reliable, industrial-scale production with competitive cost and performance.

7. Conclusion

Recent studies have demonstrated the successful synthesis of Zeolite X from diverse industrial wastes, including coal fly ash (CFA), granite stone sludge (GSS), rice husk ash (RHA), waste porcelain, and palm oil mill fly ash (POMFA). These waste-derived zeolites exhibit promising performance in adsorption (toxic metals, CO_2, and NH_3), catalysis (hydrogen generation), and gas separation, rivaling conventional zeolites. CFA remains the most studied waste, but RHA and GSS show high potential due to their high silica content and abundance. Alkali fusion-hydrothermal synthesis is the dominant method, while microwave/ultrasound-assisted techniques reduce energy and time. Pretreatment (acid washing, magnetic separation) is critical to remove impurities and increase zeolite purity.

The downstream application of waste-derived Zeolite X directly dictates the selection of the initial precursor, optimal synthesis conditions, and post-synthetic modifications (Table 8). For gas adsorption and separation purposes, precursors like coal fly ash (CFA), spent FCC catalysts, and rice husk ash (RHA) are typically processed via high-temperature alkali fusion (823–1073 K) to dissolve inert phases into highly reactive gels, often paired with microwave crystallization to abbreviate aging time. When targeting environmental remediation, securing 100% phase purity is paramount; this necessitates multi-step pretreatments, including magnetic separation and intensive acid leaching, to completely remove iron and calcium impurities that would otherwise cause competing mineral phases. For catalysis and energy storage applications, particle grinding and calcination followed by alkaline conversion are paired with chemical impregnation to successfully load active metal phases, where the final framework Si/Al ratio and surface characteristics directly dictate hydrogen generation rates and reusability. Finally, for humidity control and thermal pump systems, natural clays and clay-waste blends undergo thermal calcination to remove organic matter, followed by liquid-phase ion exchange post-synthesis to manipulate surface framework energy and pore networks, ultimately enhancing water vapor adsorption capacity and hydrothermal stability.

When selecting waste precursors and synthesis conditions for specific target applications, clear material–process–performance relationships emerge from the reviewed literature.

- For heavy metal removal from industrial wastewater, CFA pretreated by sequential magnetic separation and acid washing, followed by alkali fusion and hydrothermal crystallization, consistently yields high-purity single-phase Zeolite X. This optimized path provides a high surface area and excellent monolayer adsorption capacities for heavy metal ions such as nickel and vanadium [15,36].
- For multi-component flue gas purification, the same CFA-derived Zeolite X synthesized via optimized calcination followed by hydrothermal treatment demonstrates highly selective adsorption of ammonia and sulfur dioxide at room temperature. This approach outperforms other gas species through a specific framework bridging oxygen interactions confirmed by molecular modeling [42].
- For carbon dioxide capture, Zeolite X co-synthesized from rice husk ash (RHA) and coal ash—taking advantage of the high-purity amorphous silica content inherent to agricultural biomass-achieves a superior surface area and enhanced gas capture capacity compared to routes utilizing coal fly ash alone [17].
- Finally, for ammonia gas adsorption requiring long-term cycling stability, a non-magnetic CFA fraction processed via high-temperature fusion followed by hydrothermal treatment is preferred over commercial alternatives. This material exhibits a lower desorption temperature, which enables highly energy-efficient regeneration and maintains strong recycling efficiency across consecutive adsorption–desorption cycles [15].

Table 8
Most important conclusions.

Target application	Best Waste Materials (precursors)	Optimal synthesis condition	Key Operational Insights	Ref
Gas Adsorption & Separation	Coal Fly Ash (CFA), Spent FCC Catalysts, Rice Husk Ash (RHA)	Alkali fusion with at high temperatures (823–1073 K), followed by conventional or microwave-assisted hydrothermal crystallization	Fusion breaks down inert waste phases to create highly reactive gels. Microwave synthesis significantly cuts crystallization time down to 60 min.	[15, 17, 34, 42, 56]
Environmental Remediation	Granite Stone Sludge (GSS), Coal Fly Ash (CFA), Crushed Stone Powder	Multi-step pretreatment (magnetic separation and acid leaching with or followed by aging (up to 24 h) and hydrothermal synthesis.	Complete removal of iron and calcium impurities during pretreatment is mandatory to prevent competing mineral phases and ensure 100% phase purity.	[21, 30, 36, 41]
Catalysis & Energy Storage	Coal Fly Ash (CFA), Coal-Fired Slag (CFS)	Particle grinding and calcination, followed by alkaline conversion and subsequent chemical impregnation/reduction to load active metal phases.	The final framework Si/Al ratio and surface characteristics directly control the hydrogen generation rates and guarantee high structural reusability.	[13, 35, 43, 65]
Humidity Control & Thermal Pumps	Natural Clays, Clay-Waste Blends, Rice Husk Ash (RHA)	Thermal calcination of raw clay/ash to remove organic matter, followed by liquid-phase ion exchange post-synthesis	Cation substitution safely modifies the surface framework energy and pore features, drastically boosting water vapor adsorption and hydrothermal stability.	[57, 58, 60]

The reviewed studies demonstrate that waste-derived Zeolite X is gaining increasing attention as a sustainable material, with ongoing efforts directed toward process optimization, the integration of AI-driven modeling for synthesis control, and the expansion of applications in environmental and energy technologies. By addressing these challenges, waste-derived Zeolite X has the potential to become a cost-effective, sustainable alternative to conventional zeolites, supporting circular economy goals in pollution control and clean energy.

Funding information

Alenka Ristić acknowledges the financial support of the Slovenian Research and Innovation Agency through the research program Nanoporous Materials (P1-0021). Alenka Ristić, Božidar Ilić and Saša Zeljković acknowledge the support of the Slovenian Research and Innovation Agency and the Ministry of Civil Affairs of Bosnia and Herzegovina through the joint bilateral research project BI-BA/24-25-020 (19/6-020/966-13-1/23), entitled "Circular Economy: Application of Waste Raw Materials in Zeolite Synthesis" between Bosnia and Herzegovina and the Republic of Slovenia (2024–2025).

CRediT authorship contribution statement

Božidar Ilić: Writing – original draft, Resources, Investigation, Data curation, Conceptualization. **Alenka Ristić:** Writing – review & editing, Visualization, Validation, Supervision, Resources, Conceptualization. **Saša Zeljković:** Writing – original draft, Supervision, Resources, Project administration, Formal analysis, Data curation, Conceptualization.

Declaration of competing interest

The authors declare that they have no known competing financial interests or personal relationships that could have appeared to influence the work reported in this paper.

Acknowledgements

A.R. acknowledges the financial support of the Slovenian Research and Innovation Agency through the research program Nanoporous Materials (P1-0021). A.R., B.I., and S.Z. acknowledge the support of the Slovenian Research and Innovation Agency and the Ministry of Civil Affairs of Bosnia and Herzegovina through the joint bilateral research project BI-BA/24-25-020 (19/6-020/966-13-1/23), Circular Economy: Application of Waste Raw Materials in Zeolite Synthesis between Bosnia and Herzegovina and the Republic of Slovenia (2024-2025).

Data availability

No data was used for the research described in the article.

References

[1] M. Slavova, I. Slavov, V. Terziev, E. Mladenova, B. Abrashev, Application of zeolite and comparable porous materials for enhancing the performance of different types of secondary batteries: a review article, J. Energy Storage 98 (2024) 112949, https://doi.org/10.1016/j.est.2024.112949.
[2] M. Yoldi, E.G. Fuentes-Ordoñez, S.A. Korili, A. Gil, Zeolite synthesis from industrial wastes, Microporous Mesoporous Mater. 287 (2019) 183–191, https://doi.org/10.1016/j.micromeso.2019.06.009.
[3] A. Hernández-Palomares, E. Ángeles-García, Y. Maldonado, E. Coutino-Gonzalez, F. Espejel-Ayala, Synthesis of industrially appealing low-silica zeolites using aluminum scraps and sand, Mater. Sci. Eng. B 307 (2024) 117508, https://doi.org/10.1016/j.mseb.2024.117508.
[4] J. Sebastian, K.M. Jinka, R.V. Jasra, Effect of alkali and alkaline earth metal ions on the catalytic epoxidation of styrene with molecular oxygen using cobalt(II)-exchanged zeolite X, J. Catal. 244 (2006) 208–218, https://doi.org/10.1016/j.jcat.2006.09.005.
[5] G.E. Christidis, H. Papantoni, Synthesis of FAU type zeolite Y from natural raw materials: hydrothermal SiO2-sinter and perlite glass, Open Mineral. J. 2 (2008) 1–5, https://doi.org/10.2174/1874456700802010001.
[6] H. Zhang, I. bin Samsudin, S. Jaenicke, G.-K. Chuah, Zeolites in catalysis: sustainable synthesis and its impact on properties and applications, Catal. Sci. Technol. 12 (2022) 6024–6039, https://doi.org/10.1039/D2CY01325H.
[7] W. Abu Jadayil, G. Shwaheen, M. Ramadan, M. Alkhedher, Beyond energy: review of innovations in green technologies for resilience and environmental sustainability, Energy Rep. 13 (2025) 5410–5426, https://doi.org/10.1016/j.egyr.2025.04.067.
[8] Z. Liang, Z. Liu, L. Yu, W. Wang, Fly ash-based zeolites: from waste to value – A comprehensive overview of synthesis, properties, and applications, Chem. Eng. Res. Des. 212 (2024) 240–260, https://doi.org/10.1016/j.cherd.2024.10.031.
[9] M.S. Araujo, D. Costa-Silva, J.C. Izidoro, D.A. Fungaro, S.M. Castanho, Zeolite synthesized from solid waste for eco-system remediation: selective adsorption in wastewater, Chemistry 7 (2025) 3, https://doi.org/10.3390/chemistry7010003.
[10] W. Zhang, T. Zhang, Y. Lv, T. Jing, X. Gao, Z. Gu, S. Li, H. Ao, D. Fang, Recent progress on the synthesis and applications of zeolites from industrial solid wastes, Catalysts 14 (2024) 734, https://doi.org/10.3390/catal14100734.
[11] R. Panek, J. Madej, L. Bandura, G. Słowik, Recycling of waste solution after hydrothermal conversion of fly ash on a semi-technical scale for zeolite synthesis, Materials 14 (2021) 1413, https://doi.org/10.3390/ma14061413.
[12] Q. Liu, J. Shang, Z. Liu, Zeolites in the epoch of catalytic recycling plastic waste: toward circular economy and sustainability, Chin. J. Catal. 71 (2025) 54–69, https://doi.org/10.1016/S1872-2067(24)60273–1.
[13] Y. Yin, J. Wu, X. Wang, K. Ma, W. Zhai, Z. Wu, J. Zhang, Synthesis of zeolite molecular sieve 13X from coal-fired slag for efficient room temperature CO2 adsorption, Chem. Eng. Sci. 288 (2024) 119838, https://doi.org/10.1016/j.ces.2024.119838.
[14] X. Querol, N. Moreno, J.C. Umaña, A. Alastuey, E. Hernández, A. López-Soler, F. Plana, Synthesis of zeolites from coal fly ash: an overview, Int. J. Coal Geol. 50 (2002) 413–423, https://doi.org/10.1016/S0166-5162(02)00124-6.
[15] J. Lee, J. Kim, K.Y. Park, J.B. Joo, S. Bae, Enhanced and prolonged adsorption of ammonia gas by zeolites derived from coal fly ash, Chemosphere 368 (2024) 143799, https://doi.org/10.1016/j.chemosphere.2024.143799.
[16] W.W. Tu, Y.F. Zhang, J. Bai, W. Liu, Synthesis of zeolite 13X from coal fly ashes and properties of the zeolite products, Appl. Mech. Mater. 675-677 (2014) 724–727, https://doi.org/10.4028/www.scientific.net/AMM.675-677.724.
[17] Y. Jin, Q. Xu, F. Zheng, J. Lu, Enhancement in CO2 adsorption by zeolite synthesized from co-combustion ash of coal and rice husk modified with lithium ion, J. Energy Inst. 110 (2023) 101348, https://doi.org/10.1016/j.joei.2023.101348.
[18] T.F. de Aquino, S.T. Estevam, V.O. Viola, C.R.M. Marques, F.L. Zancan, L. B. Vasconcelos, H.G. Riella, M.J.R. Pires, R. Morales-Ospino, A.E.B. Torres, M. Bastos-Neto, C.L. Cavalcante, CO2 adsorption capacity of zeolites synthesized from coal fly ashes, Fuel 276 (2020) 118143, https://doi.org/10.1016/j.fuel.2020.118143.
[19] X. Ren, R. Qu, S. Liu, H. Zhao, W. Wu, H. Song, C. Zheng, X. Wu, X. Gao, Synthesis of zeolites from coal fly ash for the removal of harmful gaseous pollutants: a review, Aerosol Air Qual. Res. 20 (2020) 1127–1144, https://doi.org/10.4209/aaqr.2019.12.0651.
[20] S.S. Bukhari, J. Behin, H. Kazemian, S. Rohani, Conversion of coal fly ash to zeolite utilizing microwave and ultrasound energies: a review, Fuel 140 (2015) 250–266, https://doi.org/10.1016/j.fuel.2014.09.077.
[21] P. Mohammadi, N. Mirghaffari, Z. Razavi, M. Soleimani, Synthesis and characterization of zeolite X from granite stone sludge, Mater 6 (2025) 100466, https://doi.org/10.1016/j.nxmate.2024.100466.
[22] H.M. Galindo Valbuena, A.F. Medina, J.C. Vargas, O.H. Fandiño, Synthesis of zeolites Na-A, Na-X, and analcime from crushed stone waste and their applications in heavy metal removal in aqueous media, Chem. Eng. Res. Des. 197 (2023) 159–172, https://doi.org/10.1016/j.cherd.2023.07.018.
[23] V. Gargiulo, F. Di Natale, M. Alfe, From agricultural wastes to advanced materials for environmental applications: rice husk-derived adsorbents for heavy metals removal from wastewater, J. Environ. Chem. Eng. 12 (2024) 113497, https://doi.org/10.1016/j.jece.2024.113497.
[24] T. Wajima, Y. Ikegami, Synthesis of crystalline zeolite–13X from waste porcelain using alkali fusion, Ceram. Int. 35 (2009) 2983–2986, https://doi.org/10.1016/j.ceramint.2009.03.014.
[25] I. El Bojaddayni, M.E. Küçük, Y. El Ouardi, I. Jilal, S. El Barkany, K. Moradi, E. Repo, K. Laatikainen, A. Ouammou, A review on synthesis of zeolites from natural clay resources and waste ash: recent approaches and progress, Miner. Eng. 198 (2023) 108086, https://doi.org/10.1016/j.mineng.2023.108086.
[26] H. Koshlak, Synthesis of zeolites from coal fly ash using alkaline fusion and its applications in removing heavy metals, Materials 16 (2023) 4837, https://doi.org/10.3390/ma16134837.
[27] X. Lu, W. Zhou, C. Qi, M. Yang, Enhanced plant restoration in open-pit mines using maize straw and ultrasonically pre-treated coal fly ash, Sustainability 12 (2020) 9307, https://doi.org/10.3390/su12229307.
[28] N. Na chat, S. Sangsuradet, P. Tobarameekul, P. Worathanakul, Modified hierarchical zeolite X derived from riceberry rice husk for propionic acid adsorption, Mater. Chem. Phys. 282 (2022) 125933, https://doi.org/10.1016/j.matchemphys.2022.125933.
[29] A. Kongnoo, S. Tontisirin, P. Worathanakul, C. Phalakornkule, Surface characteristics and CO2 adsorption capacities of acid-activated zeolite 13X prepared from palm oil mill fly ash, Fuel 193 (2017) 385–394, https://doi.org/10.1016/j.fuel.2016.12.087.
[30] S. Kuroki, T. Hashishin, T. Morikawa, K. Yamashita, M. Matsuda, Selective synthesis of zeolites A and X from two industrial wastes: crushed stone powder and aluminum ash, J. Environ. Manag. 231 (2019) 749–756, https://doi.org/10.1016/j.jenvman.2018.10.082.
[31] S. Zeljković, T. Ivas, Synthesis of zeolite and carbon-zeolite composite from waste silica fumes, in: Proceedings of the Slovenian Chemical Society (Si-Za), 2024, pp. 1–2. https://si-za.si/10-ssh-symposium-on-zeolites/book-of-papers/.
[32] C. Han, J. Yang, S. Dong, L. Ma, Q. Dai, J. Guo, Zeolite preparation from industrial solid waste: current status, applications, and prospects, Sep. Purif. Technol. 354 (2025) 128957, https://doi.org/10.1016/j.seppur.2024.128957.
[33] M. Yoldi, E.G. Fuentes-Ordoñez, S.A. Korili, A. Gil, Zeolite synthesis from aluminum saline slag waste, Powder Technol. 366 (2020) 175–184, https://doi.org/10.1016/j.powtec.2020.02.069.

[34] P. Truttim, S. Asavapisit, R. Piyaphanuwat, Microwave synthesis of zeolite X from bituminous fly ash and its characterization, Mater. Today Proc. (2023), https://doi.org/10.1016/j.matpr.2023.06.023.
[35] C. Bilgiç, S. Hoşgün, A. Çiftci, Hydrothermal synthesis and characterization of zeolite A and zeolite X from kaolinite, fly ash, slag and their application in hydrogen generation systems on NaBH4 hydrolysis, Int. J. Hydrog. Energy 109 (2025) 742–752, https://doi.org/10.1016/j.ijhydene.2025.02.171.
[36] A.A. Marhoon, S.A. Hasbullah, N. Asikin-Mijan, W.N.A.W. Mokhtar, Hydrothermal synthesis of high-purity zeolite X from coal fly ash for heavy metal removal: kinetic and isotherm analysis, Adv. Powder Technol. 34 (2023) 104242, https://doi.org/10.1016/j.apt.2023.104242.
[37] J.-C. Kim, M. Choi, H.J. Song, J.E. Park, J.-H. Yoon, K.-S. Park, C.G. Lee, D.-W. Kim, Synthesis of uniform-sized zeolite from windshield waste, Mater. Chem. Phys. 166 (2015) 20–25, https://doi.org/10.1016/j.matchemphys.2015.09.028.
[38] X. Zhao, H. Wang, Y. Wang, L. Xue, B. Xiao, X. Zhang, Z. Zhou, Q. Wang, An oil shale ash-based X-type zeolite with rapid and high-capacity Cd2+ adsorption, Mater. Lett. 394 (2025) 138601, https://doi.org/10.1016/j.matlet.2025.138601.
[39] X. Xu, K. Chen, Y. Dai, X. Xing, L. Sun, Synthesis of zeolite A–X from coal fly ash via Ultrasonic-Alkali fusion hydrothermal method for the efficient removal of Cr (VI) from wastewater, Water. Air. Soil Pollut. 236 (2025) 137, https://doi.org/10.1007/s11270-025-07774-w.
[40] C. Belviso, F. Cavalcante, A. Lettino, S. Fiore, Effects of ultrasonic treatment on zeolite synthesized from coal fly ash, Ultrason. Sonochem. 18 (2011) 661–668, https://doi.org/10.1016/j.ultsonch.2010.08.011.
[41] Q. Yao, Y. Peng, M. Chen, Y. Wang, J. Ding, B. Ma, Q. Wang, S. Lu, One-step high efficiency synthesis of zeolite from fly ash by mechanochemical method as a low-cost adsorbent for cadmium removal, J. Environ. Chem. Eng. 12 (2024) 111877, https://doi.org/10.1016/j.jece.2024.111877.
[42] R. Dai, Y. Zhao, Q. Zhai, S. Wang, H. Li, X. Chen, J. Yu, J. Dou, Exploring adsorption behaviors of NO, NH3, SO2, CO2, C7H8 from flue gases on X-zeolite derived from coal fly ash: experimental and micro-calculation, Colloids Surf. Physicochem. Eng. Asp. 716 (2025) 136716, https://doi.org/10.1016/j.colsurfa.2025.136716.
[43] Y. Cui, A.P. Baker, X. Xu, Y. Xiang, L. Wang, M. Lavorgna, J. Wu, Enhancement of Nafion based membranes for direct methanol fuel cell applications through the inclusion of ammonium-X zeolite fillers, J. Power Sources 294 (2015) 369–376, https://doi.org/10.1016/j.jpowsour.2015.06.078.
[44] Y. Liu, Z.-W. Zhao, C. Zhang, W.-Z. Jiao, Y.-Z. Liu, Synthesis of zeolite X from fly ash in an impinging stream reactor and its mechanisms, Chem. Eng. Sci. 294 (2024) 120123, https://doi.org/10.1016/j.ces.2024.120123.
[45] S. Boycheva, D. Zgureva, H. Lazarova, M. Popova, Comparative studies of carbon capture onto coal fly ash zeolites Na-X and Na–Ca-X, Chemosphere 271 (2021) 129505, https://doi.org/10.1016/j.chemosphere.2020.129505.
[46] J. Hayfron, S. Jääskeläinen, S. Tetteh, Synthesis of zeolite from rice husk ash and kaolinite clay for the removal of methylene blue from aqueous solution, Heliyon 11 (2025) e41325, https://doi.org/10.1016/j.heliyon.2024.e41325.
[47] P. Kunecki, E. Wisła-Walsh, K. Kornaus, P. Gara, M. Wdowin, Assessment of silver modification's impact on the internal structure stability, phase and textural properties of fly ash-derived X and A zeolites, Mater. Chem. Phys. 339 (2025) 130730, https://doi.org/10.1016/j.matchemphys.2025.130730.
[48] M.T. Ritter, M.Á. Lobo-Recio, I. Padilla, M. Romero, A. López-Delgado, Salt slag and rice husk ash as raw materials in zeolite synthesis: process optimization using central composite rotational design, Sustain. Chem. Pharm. 39 (2024) 101599, https://doi.org/10.1016/j.scp.2024.101599.
[49] J. Shi, Q. Wu, X. Meng, F.-S. Xiao, Sustainable synthesis of zeolites, Microporous Mesoporous Mater. 403 (2026) 114017, https://doi.org/10.1016/j.micromeso.2025.114017.
[50] A.M. Alotaibi, An overview of zeolites: from historical background to diverse applications, Molecules 30 (2025) 4036, https://doi.org/10.3390/molecules30204036.
[51] J.E. Schmidt, G.T. Whiting, A.D. Chowdhury, B. Seoane, B.M. Weckhuysen, Spectroscopy of zeolites, (2017). https://doi.org/10.1039/9781788010610-00240.
[52] M. Hartmann, M. Thommes, W. Schwieger, Hierarchically-ordered zeolites: a critical assessment, Adv. Mater. Interfaces 8 (2021) 2001841, https://doi.org/10.1002/admi.202001841.
[53] G. Yao, J. Lei, X. Zhang, Z. Sun, S. Zheng, One-step hydrothermal synthesis of zeolite X powder from natural low-grade diatomite, Materials 11 (2018) 906, https://doi.org/10.3390/ma11060906.
[54] S.H. van Vreeswijk, B.M. Weckhuysen, Emerging analytical methods to characterize zeolite-based materials, Natl. Sci. Rev. 9 (2022) nwac047, https://doi.org/10.1093/nsr/nwac047.
[55] A. Khaleque, M.M. Alam, M. Hoque, S. Mondal, J.B. Haider, B. Xu, M.A.H. Johir, A. K. Karmakar, J.L. Zhou, M.B. Ahmed, M.A. Moni, Zeolite synthesis from low-cost materials and environmental applications: a review, Environ. Adv. 2 (2020) 100019, https://doi.org/10.1016/j.envadv.2020.100019.
[56] B. Wang, H. Chen, S. Wang, H. Pan, Z. Yang, H. Su, H. Zhang, J. Pan, J.-N. Zhang, L. Li, Q. Pan, W. Yan, Synthesis of customized zeolite X with outstanding CO2 selectivity over CH4 and N2 using facile activated spent fluid catalytic cracking catalysts, Sep. Purif. Technol. 354 (2025) 128713, https://doi.org/10.1016/j.seppur.2024.128713.
[57] X. He, B. Xue, R. Wei, K. Liao, G. Li, T. Zhao, A novel hydrophobic shell of bio-based polyurethane coated on zeolite 13X: for designing a high-efficiency adsorption heat pump, Energy Convers. Manag. 313 (2024) 118612, https://doi.org/10.1016/j.enconman.2024.118612.
[58] F.D.S. Feudjio, C.G. Fotsop, D.R.T. Tchuifon, J.N. Ndi, R.A. Ntieche, H.M. Ngomo, M. Yılmaz, Tunable water vapor adsorption properties on ion exchange microporous zeolite Na-X derived from natural kaolin, Inorg. Chem. Commun. 177 (2025) 114379, https://doi.org/10.1016/j.inoche.2025.114379.
[59] A.R. Shrotri, A.R. Birje, P.S. Niphadkar, V.V. Bokade, N.A. Mali, S.U. Nandanwar, Performance of Li exchange hierarchical X zeolite for CO2 adsorption and H2 separation, J. Ind. Eng. Chem. 133 (2024) 505–514, https://doi.org/10.1016/j.jiec.2023.12.027.
[60] Q. Xu, J. Lu, Z. Zhou, Y. Jin, FAU zeolites from coal/rice husk co-combustion ash (co-ash) for CO2 adsorption: synthesis, characterization, adsorption and regeneration performance, Sep. Purif. Technol. 369 (2025) 133147, https://doi.org/10.1016/j.seppur.2025.133147.
[61] The effect of crystallization and aging time in zeolite synthesis using coal fly ash as silica and alumina source | Jurnal Teknologi (Sciences & Engineering), (n.d.). https://journals.utm.my/jurnalteknologi/article/view/22254 (accessed June 5, 2026).
[62] Q. Zeng, Z. Jia, X. Liu, Y. Fan, Y. Pang, J. Cheng, Hydrazine vapor modified waste molecular sieves to reconstitute 13X zeolites for efficient wide scale domain CO2 capture, J. Environ. Chem. Eng. 13 (2025) 115861, https://doi.org/10.1016/j.jece.2025.115861.
[63] L. Cao, Y. Zuo, S. Liang, Y. Sun, Y. Ke, J. Yang, X. Wei, J. Hu, H. Hou, Geopolymerization of MSWI fly ash and coal fly ash for efficient solidification of heavy metals: insights into stabilization mechanisms and long-term leaching behavior, Constr. Build. Mater. 411 (2024) 134359, https://doi.org/10.1016/j.conbuildmat.2023.134359.
[64] X. Gao, S. Deng, S. Kawi, Zeolite-based catalytic membrane reactors for thermo-catalytic conversion of CO2, iScience 25 (2022) 105343, https://doi.org/10.1016/j.isci.2022.105343.
[65] R.C.P. Oliveira, M. Vasić, D.M.F. Santos, B. Babić, R. Hercigonja, C.A.C. Sequeira, B. Šljukić, Performance assessment of a direct borohydride-peroxide fuel cell with Pd-impregnated faujasite X zeolite as anode electrocatalyst, Electrochim. Acta 269 (2018) 517–525, https://doi.org/10.1016/j.electacta.2018.03.021.
[66] K.L.T. Nguena, C.G. Fotsop, S.B.L. Ngomade, A.K. Tamo, C.A. Madu, F. Ezema, E. E. Oguzie, Mathematical modeling approach for the green synthesis of high-performance nanoporous zeolites Na-X optimized for water vapor sorption, Mater. Today Commun. 37 (2023) 107406, https://doi.org/10.1016/j.mtcomm.2023.107406.
[67] A. Jiménez, R. Trujillano, V. Rives, M.A. Vicente, A. Gil, Removal of heavy metals from aqueous solutions by adsorption on zeolites synthesized from aluminum saline slags, Inorg. Chem. Commun. 170 (2024) 113440, https://doi.org/10.1016/j.inoche.2024.113440.
[68] H. Chen, Y.J. Zhang, P.Y. He, C.J. Li, Cost-effective and facile one step synthesis of ZSM-5 from silica fume waste with the aid of metakaolin and its NOx removal performance, Powder Technol. 367 (2020) 558–567, https://doi.org/10.1016/j.powtec.2020.04.014.
[69] R. Jamal, Y. Ue, M. Miyamoto, Y. Oumi, S. Uemiya, Conversion of biomass combustion ash to zeolites by low-temperature alkali fusion method, Next Res. 2 (2025) 100359, https://doi.org/10.1016/j.nexres.2025.100359.
[70] M. Parmar, V. Shukla, M. Bandyopadhyay, D.K. Singh, R. Gaur, S. Shahabuddin, Synthesis of eco-friendly polyaniline-zeolite nanocomposite for pollutant remediation: empowered by robust machine learning algorithm, J. Clean. Prod. 470 (2024) 143339, https://doi.org/10.1016/j.jclepro.2024.143339.
[71] C. Cao, W. Xuan, S. Yan, Q. Wang, Zeolites synthesized from industrial and agricultural solid waste and their applications: a review, J. Environ. Chem. Eng. 11 (2023) 110898, https://doi.org/10.1016/j.jece.2023.110898.
[72] Z. Mahdi, A.E. Hanandeh, C. Pratt, N. Ordou, Harnessing the potential of manufactured zeolites for a sustainable circular economy, J. Ecol. Eng. 27 (2026) 1–22, https://doi.org/10.12911/22998993/211815.